THE ROLE OF 15-LOX-1 IN RESISTANCE TO CHEMOTHERAPEUTICS

A THESIS SUBMITTED TO
THE GRADUATE SCHOOL OF NATURAL AND APPLIED SCIENCES
OF
MIDDLE EAST TECHNICAL UNIVERSITY

BY

HASAN HÜSEYİN KAZAN

IN PARTIAL FULFILLMENT OF THE REQUIREMENTS
FOR
THE DEGREE OF DOCTOR OF PHILOSOPHY
IN
BIOLOGY

JANUARY 2020

Approval of the thesis:

THE ROLE OF 15-LOX-1 IN RESISTANCE TO CHEMOTHERAPEUTICS

submitted by **HASAN HÜSEYİN KAZAN** in partial fulfillment of the requirements for the degree of **Doctor of Philosophy** in **Biology, Middle East Technical University** by,

Prof. Dr. Halil Kalıpçılar
Dean, Graduate School of **Natural and Applied Sciences**

       _____

Prof. Dr. Ayşe Gül Gözen
Head of Department, **Biology**

       _____

Prof. Dr. Ufuk Gündüz
Supervisor, **Biology Dept., METU**

       _____

Assoc. Prof. Dr. Pelin Mutlu
Co-supervisor, **Central Lab. Mol. Bio. Biotech., METU**

       _____

Examining Committee Members:

Prof. Dr. Sreeparna Banerjee
Biology Dept., METU

       _____

Prof. Dr. Ufuk Gündüz
Biology Dept., METU

       _____

Prof. Dr. Özlem Darcansoy İşeri
Molecular Biology and Genetics Dept., Başkent University

       _____

Prof. Dr. Mehmet Ali Ergün
Medical Genetics Dept., Gazi University

       _____

Assoc. Prof. Dr. Çağdaş Devrim Son
Biochemistry Dept., METU

       _____

Date: 30.01.2020

I hereby declare that all information in this document has been obtained and presented in accordance with academic rules and ethical conduct. I also declare that, as required by these rules and conduct, I have fully cited and referenced all material and results that are not original to this work.

Name, Last name : Hasan Hüseyin Kazan

Signature :

ABSTRACT

THE ROLE OF 15-LOX-1 IN RESISTANCE TO CHEMOTHERAPEUTICS

Kazan, Hasan Hüseyin
Doctor of Philosophy, Biology
Supervisor : Prof. Dr. Ufuk Gündüz
Co-Supervisor: Assoc. Prof. Dr. Pelin Mutlu

January 2020, 104 pages

Chemotherapy is one of the best options to treat cancer. However, drug resistance can limit the efficacy of chemotherapeutics. There have been several reasons for the cancer drug resistance including the export of the drug from cells, inactivation of drugs by enzymatic processes, mutations that limit the binding of the drugs to the target proteins, resistance to cell death mechanism by cellular manipulations and reorganization of the cell membrane.

15-Lipoxygenase-1 (15-LOX-1) is a member of the lipoxygenase family containing iron and catalysing oxygenation of the polyunsaturated fatty acids. Due to this role, 15-LOX-1 is involved in the regulation of critical physiological conditions. However, disruption of the 15-LOX-1-mediated pathway could also trigger pathophysiological conditions, including cancer. There have been numerous reports that combine 15-LOX-1 function and cancer, and 15-LOX-1 is generally regarded as a tumour suppressor protein because of its main product that can activate the apoptosis. Although 15-LOX-1 and cancer relationship has been well defined, the role of 15-LOX-1 in cancer drug resistance has not yet been documented.

The present study aims to identify the possible involvement of the 15-LOX-1 protein and its pathways in the cancer drug resistance by focusing particularly on doxorubicin resistance. The results underlined that 15-LOX-1 was downregulated in doxorubicin-resistant cancer cells but the downregulation of 15-LOX-1 was cell and/or drug specific. Moreover, overexpression of 15-LOX-1 in doxorubicin-resistant cancer cells triggered cell death mechanisms in a cell-specific manner and partially re-sensitized the cells towards doxorubicin. Molecular studies revealed that this effect was also cell specific and was a result of cell membrane reorganization in doxorubicin-resistant MCF7 cell line. Still, further molecular and clinical studies are needed to completely explore the role of 15-LOX-1 in cancer drug resistance.

Keywords: Cancer Drug Resistance, 15-LOX-1, PPARγ, Cell Membrane Reorganization

ÖZ

Kemoterapötiklere Dirençte 15-LOX-1 Enziminin Rolü

Kazan, Hasan Hüseyin
Doktora, Biyoloji
Tez Yöneticisi: Prof. Dr. Ufuk Gündüz
Ortak Tez Yöneticisi: Doç. Dr. Pelin Mutlu

Ocak 2020, 104 sayfa

Kemoterapi kanser tedavisinde en iyi seçenekler arasındadır. Ancak ilaç dirençliliği kemoterapötiklerin etkisini sınırlayabilir. Kanserde ilaç dirençliliğinin nedenleri arasında hücrelerden ilacın hücre dışına transferi, enzimatik süreçlerle ilaçların inaktivasyonu, hedef proteinlerde ilacın bağlanmasını engelleyecek mutasyonların oluşması, hücresel manipülasyonlarla hücre ölüm mekanizmalarına direnç geliştirilmesi ve hücre membranının yeniden organizasyonu yer almaktadır.

15-Lipoksigenaz-1 (15-LOX-1), demir içeren ve çoklu sature olmayan yağ asitlerinin oksijenasyonunu katalizleyen lipoksigenaz enzim ailesinin bir üyesidir. Bu fonksiyonu sayesinde 15-LOX-1 fizyolojik olaylarda kritik roller oynar. Ancak 15-LOX-1 aracılı yolakta gerçekleşebilecek aksaklıklar kanser dahil olmak üzere birtakım patofizyolojik olayları tetikler. 15-LOX-1 aktivitesini kanserle ilişkilendiren birçok çalışma mevcuttur ve enzimin ana ürünü apoptozu tetiklediğinden 15-LOX-1 genellikle tümör baskılayıcı protein olarak kabul edilir. Kanserle 15-LOX-1 ilişkisi detaylıca açıklanmış olmasına rağmen, kanserde ilaç dirençliliğinde 15-LOX-1'in rolü bilinmemektedir.

Sunulan çalışma, özellikle doksorubisin dirençliliğine odaklanarak, kanserde ilaç dirençliliğinde 15-LOX-1 proteininin ve yolağının olası etkilerinin araştırılmasını amaçlamaktadır. Elde edilen sonuçlar, 15-LOX-1'in ekspresyonunun doksorubisine dirençli hücre hatlarında azaldığını ancak bu durumun hücre ve/veya ilaç spesifik olduğunu göstermiştir. Buna ek olarak, 15-LOX-1'in aşırı ekspresyonu, hücreler arası farklılıklar göstermekle birlikte hücre ölüm mekanizmalarını tetiklemiştir ve dirençli hücrelerin doksorubisine karşı kısmi hassasiyet geliştirmelerini sağlamıştır. Moleküler çalışmalar, bu etkinin de hücre spesifik olduğunu ve doksorubisine dirençli MCF7 hücre hattında hücre membranının yeniden organizasyonu sayesinde olduğunu göstermiştir. Yine de 15-LOX-1'in kanserde ilaç dirençliliğindeki rolünün daha detaylı aydınlatılabilmesi için ileri moleküler ve klinik çalışmalara ihtiyaç duyulmaktadır.

Anahtar Kelimeler: Kanserde İlaç Dirençliliği, 15-LOX-1, PPARγ, Hücre Membranı Organizasyonu

To Michael Faraday

ACKNOWLEDGMENTS

TABLE OF CONTENTS

xiii

LIST OF TABLES

LIST OF FIGURES

FIGURES

LIST OF ABBREVIATIONS

DNA	Deoxyribonucleic acid
RNA	Ribonucleic acid
shRNA	Short hairpin RNA
mRNA	Messenger RNA
cDNA	Complementary DNA
LOX	Lipoxygenase
15-LOX-1	15-Lipoxygenase-1
PPARγ	Peroxisome proliferator-activated receptor gamma
ERK	Extracellular Signal-Regulated Kinase 2
NF-κB	Nuclear factor-kappa B
P-gp	P-glycoprotein
MDR1	Multidrug resistance protein 1
ATP	Adenosine triphosphate
13(S)-HODE	13-Hydroxyoctadecadienoic acid
PUFA	Polyunsaturated fatty acid
PBS	Phosphate buffered saline
OD	Optical density
DOX	Doxorubicin
ZOL	Zoledronic acid

DMSO	Dimethyl sulfoxide
ETO	Etoposide
PAGE	Polyacrylamide gel electrophoresis
SDS	Sodium dodecyl sulphate
TBS	Tris buffer saline
TBST	Tris buffer saline-Tween 20
ELISA	Enzyme-linked immunosorbent assay
PCR	Polymerase chain reaction
qRT-PCR	Quantitative reverse transcriptase PCR
GC/MS	Gas chromatography/ Mass spectrometry

CHAPTER 1

INTRODUCTION

1.1 Cancer Treatment and Cancer Drug Resistance

Cancer is one of the major pathological conditions causing a high rate of mortality (American Cancer Society, 2017; World Health Organization, 2017). It is natural or unnatural results of cellular modifications including DNA mutations affecting the protein function, chromosomal translocations, DNA instability, epigenetic changes, alterations in hormone levels, free radicals, reactive lipid and oxygen species generated by metabolic events, immune system activation or suppression, viral, bacterial, and/or fungal infections, radiation and smoking (Bertram, 2001; Rieger, 2004; American Cancer Society, 2017).

The properties of carcinogenesis, also called the hallmarks of cancer, could be listed as self-sufficiency in cell proliferation, activation of invasive and metastatic ability, insensitivity to growth suppressors, replicative immortality, sustained angiogenesis, evasion of cell death, deregulated energy metabolism and modulation of immune system (Hanahan and Weinberg, 2000; Hanahan and Weinberg, 2011).

Surgery, radiation therapy, immune therapy, and chemotherapy are the major approaches for cancer treatment. These approaches may be combined to increase the efficacy according to the parameters including tumour size and localization, metastases, and stage of cancer (American Cancer Society, 2017).

Chemotherapy is generally the most frequently applied approach to fight against cancer and chemotherapeutic drugs are administered to the patients as a single treatment strategy and/or after surgery to prevent the relapse. There are numerous anti-cancer drugs that target diverse critical compartments of the cellar mechanisms

1

to inhibit cancer cell proliferation. One of these drugs is doxorubicin which is widely used for the treatment of particularly breast cancer (O'Shaughnessy, 2005; Glück, 2005).

Although chemotherapy is regarded as the best option for most cases, the resistance to the drugs used during the therapy is the major obstacle preventing the treatment of the cancer. Drug resistance is the term which defines the mechanisms by which the tumour cells inhibit the cytotoxic effects of the drugs in a cellular or systemic perspective (Simon and Schindler, 1994). The resistance could be intrinsic or developed in an acquired manner (Krishna and Mayer, 2000; Ejendal and Hrycyna, 2002). Drug resistance is the primary factor limiting the efficacy of the chemotherapeutics to treat cancer (Longley and Johnston, 2005).

In the cellular context, cancer drug resistance could be a result of several factors, including efflux of drug from cytoplasm by ATP-binding cassette (ABC) family transporter proteins, conversion of the drug to non-toxic forms by specific cellular enzymes, activation of detoxification system by the cell, blockage of protein active sites targeted by the drugs via DNA mutations, alterations in the protein localization that prevent to be targeted by the drugs, induction of DNA repair mechanism that diminish the role of the drugs targeting cell cycle, prevention of cell death mechanisms and modification of the cell membrane components (Figure 1.1; Gottesman et al, 2002; Longley and Johnston, 2005; Holohan et al 2013; Housman et al 2014; Panda and Biswal, 2019).
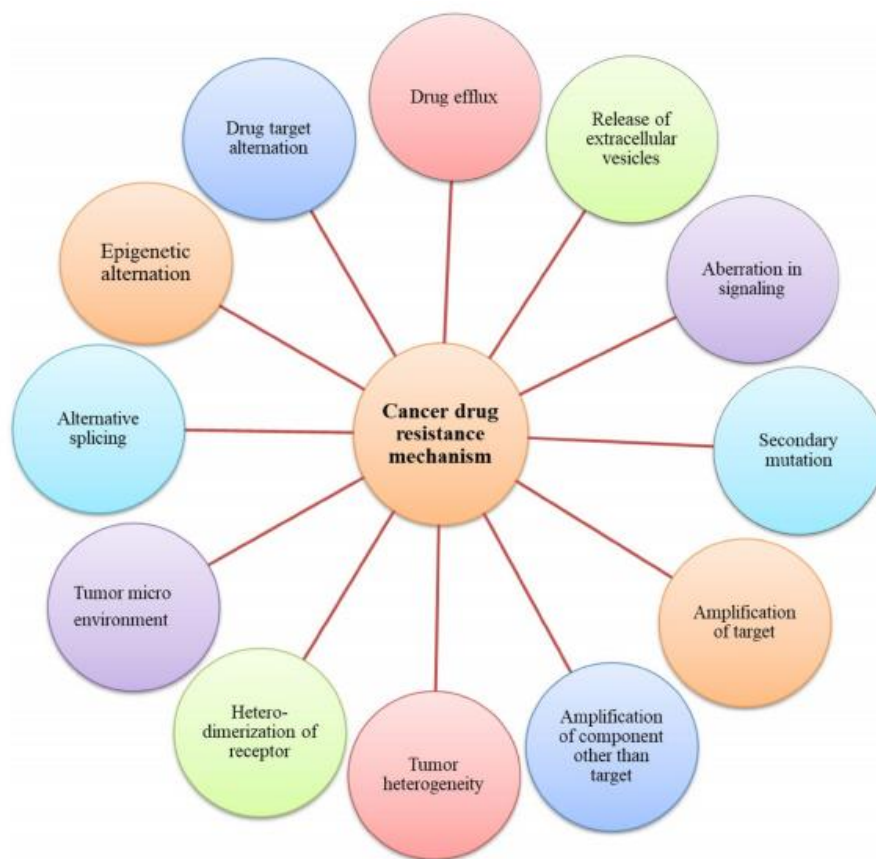
Figure 1-1. Mechanisms responsible for cancer drug resistance (Panda and Biswal, 2019).

1.2   Cell membrane modifications in cancer drug resistance

Multidrug resistance is the most common type of cancer drug resistance. One of the best-known mechanisms is the overexpression of P-glycoprotein (P-gp). P-gp is a membrane-bound protein and displays a role as a drug efflux protein using ATP. ATP is critical in terms of P-gp function and P-gp acts a drug-dependent ATPase (Bosch and Croop, 1996; Keppler, 2011).

Although expression of P-gp was associated with cancer drug resistance, MDR1 transfection may not confer the resistance phenotype. This could be a result of other mechanisms modulating the function of P-gp instead of its expression alone (Lavie and Liscovitch, 2001).

3

One of the major factors affecting the function of the P-gp is lipid composition of cell membrane. Lipids act a critical role in drug transportation and P-gp activity by modulating the membrane fluidity (Leibovici et al., 1996). The substrates of P-gp interact with membrane lipids to reach the P-gp itself (Higgins and Gottesman, 1992). Additionally, P-gp must be reconstituted for intact activity with the involvement of membrane lipids, particularly unsaturated phosphatidylcholine, phosphatidylserine and saturated phosphatidylethanolamine for ATPase activity (Lavie and Liscovitch, 2001). Alas, lipids have been shown to have a role in drug binding to P-gp (Urbatsch and Senior, 1995).

The studies reported that the membrane fluidity was controversial in terms of limiting the function of P-gp. Still, membrane lipids especially cholesterol, glycosphingolipids and other lipids such as arachidonic acid, docosahexaenoic acid and sphingomyelin were the critical lipids altered in resistant cells (Lavie and Liscovitch, 2001).

The membrane lipids have different chemical structures and volumes. Thus, alterations in the membrane lipid compositions could result in changes in the membrane permeability and curvature. Membrane biophysics are fundamentally influenced by the acyl chain saturation of fatty acids and lipids. Thus, saturation of acyl chains is critical for membrane fluidity and dynamics. In addition, the length of acyl chains is also important for interaction with transmembrane protein; therefore, it affects the membrane thickness and dynamics (Figure 1.2; Peetla et al., 2013).
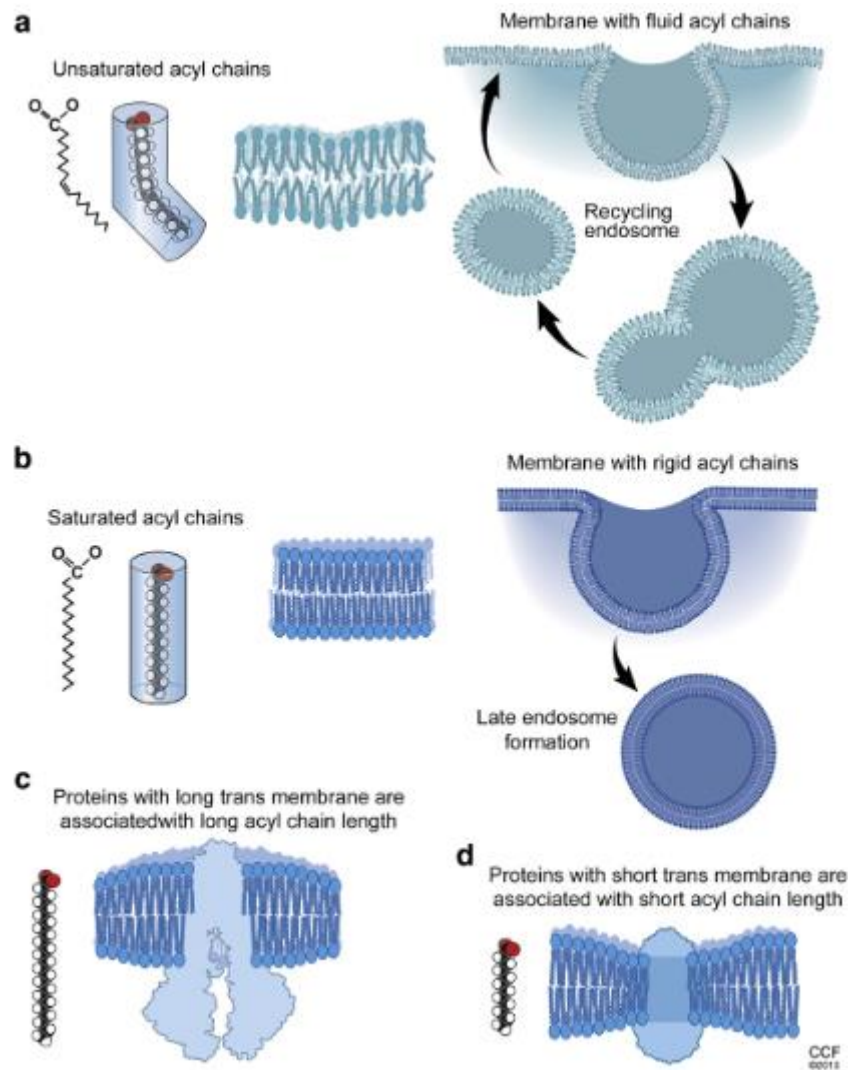
Figure 1-2 Effects of acyl chains on membrane dynamics. a) Unsaturated phospholipids can increase the permeability of cell membrane. b) Saturated phospholipids promote order membrane structure and limits the permeability. c) Long acyl chain lipids associate with long proteins, increasing the thickness of the membrane while d) short transmembrane domain-containing proteins interact with short acyl chain, decreasing the thickness of the cell membrane (Peetla et al., 2013).

In addition to the effect on P-gp activity, lipid profile of the cell membrane could determine the intracellular drug accumulation. Most chemotherapeutics are weak bases and regarded to transverse the cell membrane (Mayer et al., 1987). Hence, membrane biophysics are critical for drug influx. The studies underlined that the

drug-resistant cell lines have an altered membrane lipid profile when the drug influx was limited in those cells. The membrane dynamics in this effect contain membrane fluidity, membrane potential, structural deviations, lipid density or the combination of these factors (Hendrich and Michalak, 2003; Palleres-Trujillo et al., 2000).

The importance of membrane lipids on P-gp function was demonstrated by using the yeast membrane bilayer and purified P-gp in detergent layer, where the affinity of the drugs was higher in the yeast membrane than that in the detergent (Jin et al., 2012).

In a study in which a breast cancer cell line, MCF7, and its doxorubicin-resistant counterpart were used, the lipid profiles of the cells were deviated upon gaining resistance to the drug. The rigidity analyses proved that the membranes of the resistant cells were more rigid compared to sensitive cells due to altered membrane lipids. Moreover, the doxorubicin was showed to be trapped in lipid bilayer in resistant cells, underlying the resistance mechanism (Figure 1.3; Peetla et al., 2010).
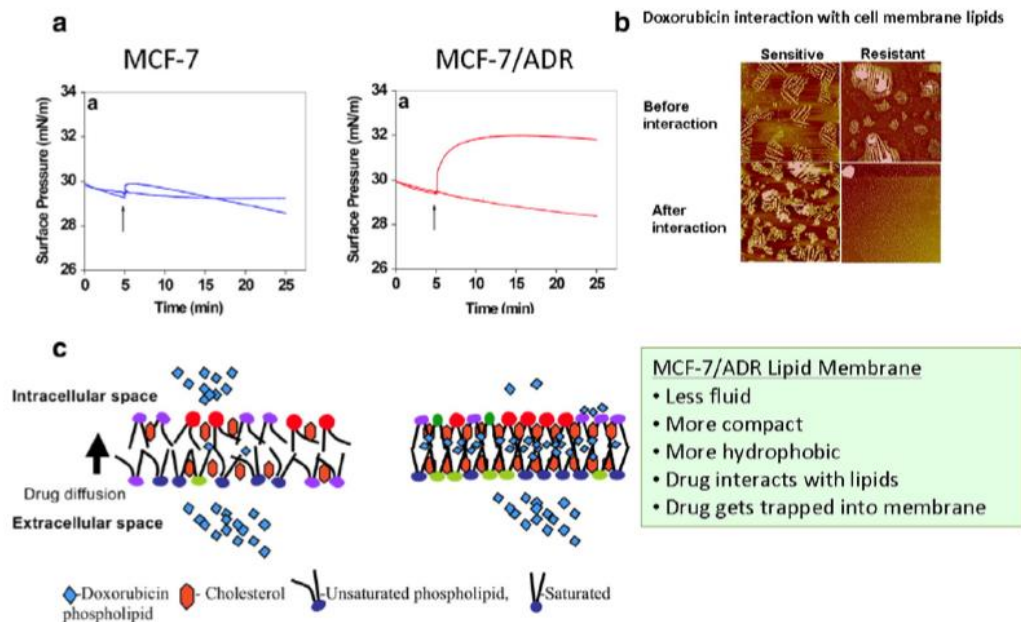
Figure 1-3 Membrane biophysics in sensitive and doxorubicin-resistant MCF7 cells. a) Doxorubicin interacted strongly with lipids in doxorubicin-resistant MCF7 cells, which was also confirmed by b) AFM images. c) Illustration of doxorubicin trapping in the lipid bilayer and the mechanisms related to lipid bilayer-dependent resistance status of doxorubicin-resistant cell line (Peetla et al., 2013).

P-gp function was proved to be affected by lipid composition in drug resistance (Ferte, 2000; Clay and Sharom, 2013). P-gp is a long protein affecting the membrane thickness by interacting with long acyl chains. The thickness of the membrane limits the drug transfer into the cells (Figure 1.4; Peetla et al., 2013).
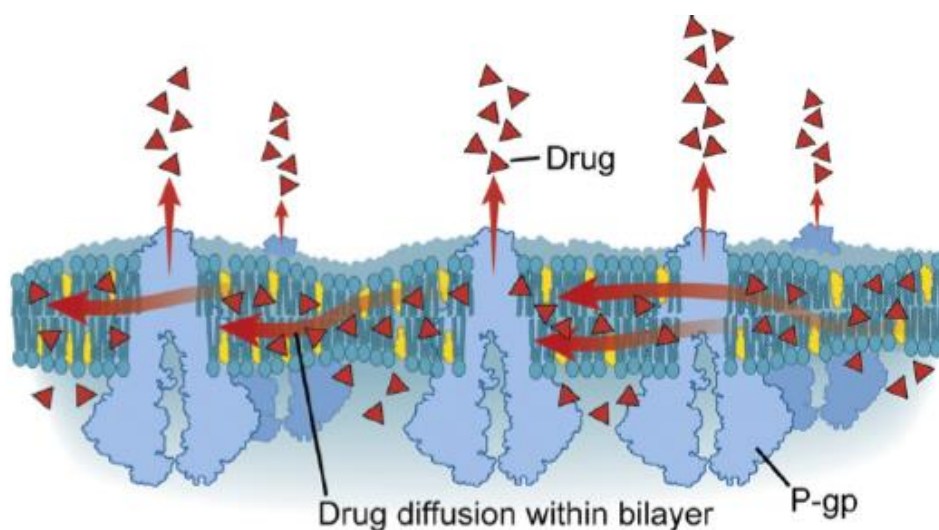
Figure 1-4 Effect of P-gp on cell thickness and drug diffusion within the membrane bilayer (Peetla et al., 2013).

The membrane lipids also crosstalk with the oxidative stress. The reactive intermediates produced by the oxidative stress could result in lipid peroxidation of polyunsaturad fatty acids and form lipoperoxyl radical which reacts with a lipid and create a lipid radical and hydroperoxide. The breakage of lipids and the formation of lipid peroxidation could alter the permeability and fluidity of the membrane and finally influence the cancer drug resistance (Barrera, 2012; Baran et al., 2011).

1.3   Oxidative stress, lipid peroxidation in cancer drug resistance

Altered redox status and production of reactive oxygen species (ROS) are common in cancer progression. In addition to the enzymatic processes, polyunsaturated fatty acids can be undergone lipid peroxidation process by the effects of ROS. The final product of lipid peroxidation such as 4-hydroxynonenal (HNE) can trigger apoptosis in cancer cells likewise ROS itself. However, cells may overcome the HNE or ROS-mediated death mechanisms (Figure 1.5; Barrera, 2012).

ROS are general metabolites of the cell particularly produced at the mitochondria. The cells may use the superoxide dismutases or catalases and increase the amount of

gluthatione to supress the detrimental effect of the ROS. In the excess case, ROS may interact with PUFAs and generates lipoperoxyl radicals which further processed to lipid hydroperoxide (LOOH). LOOHs are unstable but they can trigger local processes. Breakdown of the LOOHs could produce secondary messengers that induces oxidative stress. The lipid peroxidation could result in the altered membrane fluidity and permeability, which further affect the fate of the cells (Dixs and Aikens, 1993; Barrera et al., 2008).
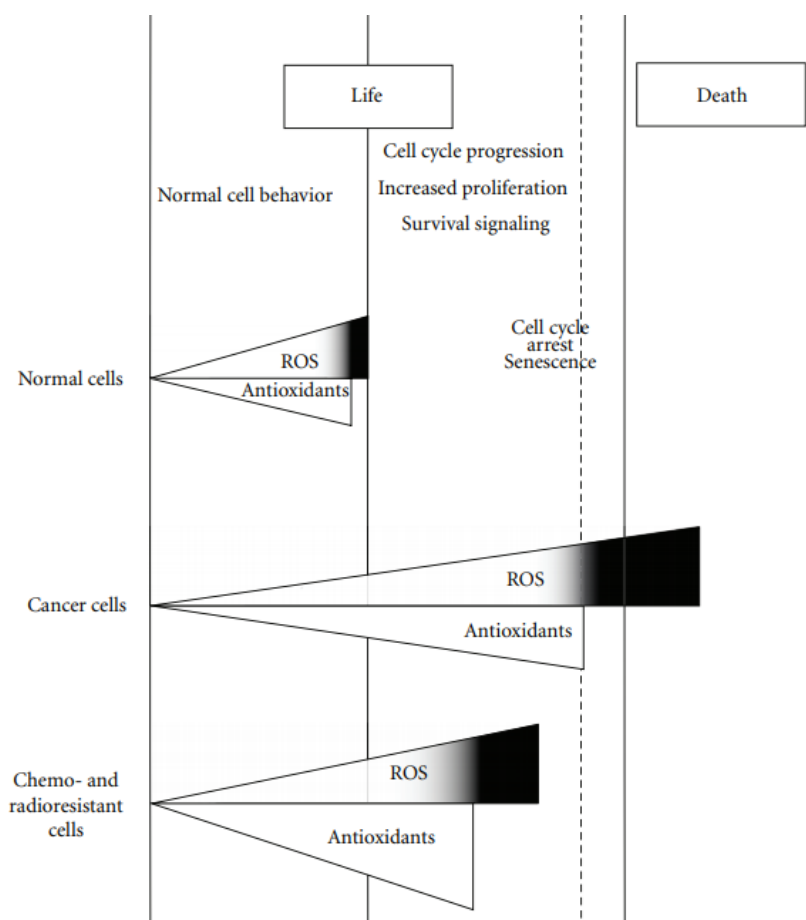
Figure 1-5 Effect of ROS on normal, cancer and therapy-resistant cancer cells (Barrera, 2012).

Studies combining cancer drug resistance and lipid peroxidation have underlined that even polyunsaturated fatty acids have been associated with the response to the drugs in cancer cells. In a study, Sturlan et al. showed that diverse cancer cells were gained

sensitivity when they treated a type of polyunsaturated fatty acids, docosahexaenoic acid (DHA) by increasing the cellular ROS and toxic lipid peroxidation products (Sturlan et al., 2003). This and similar studies could reveal that increased ROS and lipid peroxidation is a method to overcome the cancer drug resistance (Barrera, 2012).

1.4   Lipoxygenases

Lipoxygenases (LOXs) are the enzymes that catalyze the reaction to oxidize the polyunsaturated fatty acids containing minimum two isolated cis-double bonds. The members of this enzyme family contain non-heme iron to display their function. Linoleic acid and arachidonic acid are the mostly used substrates of LOX members. Generally, LOXs dioxidize free fatty acids which are very limited in cells but they can also react with the membrane-bound lipids. The membrane lipids are liberated from membrane ester lipids by cytosolic phospholipase A2 and these free fatty acids are further reacted by LOX members (Ivanov et al., 2015; Kuhn et al., 2015).

In addition to LOX members, free fatty acids such as arachidonic acid (AA), eicosapentaenoic acid (EPA) and docosahexaenoic acid (DHA) can also be reacted by cyclooxygenases (COXs) by which prostaglandins are produced. The free fatty acids are converted to hydroperoxy derivatives of the related fatty acids, which are further converted to bioactive lipid mediators including leukotrienes, lipoxins, eoxins, resolvins, hepoxilins and protectins (Haeggstrom and Funk, 2011). LOXs are especially involved in the resolution of inflammation by producing resolver lipid mediators. Also, they participate in diverse cellular and systemic pathways, drawbacks of which would be resulted in pathophysiological conditions (Ivanov et al., 2015).

The LOX members have been classified according to the oxygenation of arachidonic acid. However, this situation misled the researchers and the nomenclature turned to define the isoenzymes. There are seven LOX genes six of which encode a functional

protein. The human LOXs are named as ALOX15, ALOX15B, ALOX12, ALOX12B, ALOXE3, and ALOX5. ALOX15 is mainly expressed in eosinophils and bronchial epithelium while ALOX15B in hair roots, skin and prostate, ALOX12 in thrombocytes and skin, ALOX12B and ALOXE3 in skin and ALOX5 in leukocytes, macrophages and dendritic cells (Table 1.1; Funk et al., 2002; Kuhn et al., 2015).

Table 1-1 LOX members and tissues where they are expressed (Kuhn et al., 2015).

Human gene	Former name	Mouse gene	Former name	Major expression
ALOX15	12/15-LOX	alox15	Lc12-LOX[a]	Eosinophils, bronchial epithelium
ALOX15B	15-LOX2	alox15b	8-LOX	Hair roots, skin, prostate
ALOX12	pl12-LOX[b]	alox12	pl12-LOX	Thrombocytes, skin
ALOX12B	12R-LOX	alox12b	12R-LOX	Skin
ALOXE3	eLOX3	aloxe3	eLOX3	Skin
ALOX5	5-LOX	alox5	alox5	Leukocytes, macrophages, dendritic cells
Pseudogene		alox12e	elox12	Skin

[a] lc – leukocyte-type.
[b] pl – platelet-type.

Mammalian LOXs have a single polypeptide chain structure by which two domains are formed: N-terminal domain and C-terminal domain. N-terminal domain has parallel and anti-parallel beta-sheets while the C-terminal domain has the non-heme iron-containing catalytic domain (Gillmor et al., 19997; Choi et al., 2008).

The human lipoxygenases have different functions. ALOX12B and ALOXE3 have a role in epidermal differentiation and skin development; ALOX5 in pro-inflammatory functions; ALOX15 in erythropoiesis; ALOX12, ALOX15 and ALOX15B in anti-inflammatory functions; ALOX15 and ALOX15B in blood pressure regulation and hypertension; ALOX5, ALOX15 and ALOX15B in atherogenesis; and ALOX12 and ALOX15B in platelet function and atherothrombosis. In addition to these physiological functions, LOX members have also been associated with carcinogenesis (Kuhn et al., 2015).

1.4.1 15-Lipoxygenase-1

There are six types of human lipoxygenases that are expressed in specific tissues with different functions via metabolizing diverse substrates and producing different lipid mediators. 15-lipoxygenase-1 (15-LOX-1) is one of these enzymes and specifically uses linoleic acid as a substrate and produces 13-HODE. It is also able to produce 15-HETE via oxygenation of arachidonic acid (Figure 1.5; Ivanov et al., 2015).

15-LOX-1 has been implicated in erythropoiesis and reticulocyte maturation via maturational breakdown of mitochondria. Also, 15-LOX-1 has a role in resolution of inflammation, cardiovascular system by regulating blood pressure and hypertension, and atherogenesis in a controversial manner. 15-LOX-1 was shown to be capable of oxidizing low-density lipoproteins (LDL). However, this effect was underlined to be controversial as the modifications, both silencing and over-expression of 15-LOX-1 were linked to the atherogenesis (Kuhn et al., 2015).
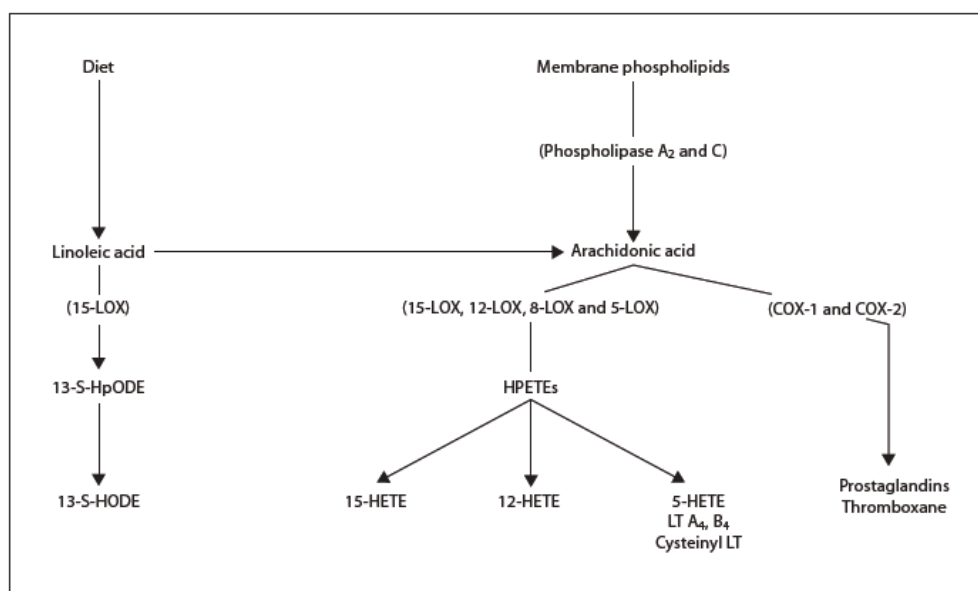
Figure 1-6 Roles of LOXs in the metabolism of the polyunsaturated fatty acids (Bhattacharya et al., 2009).

15-LOX-1 has frequently been studied in cancer. The metabolite generated by 15-LOX-1 via oxygenation of linoleic acid (13-HODE) was shown to trigger apoptosis in colorectal cancer while over-expression of 15-LOX-1 was shown to increase tumorigenesis in prostate cancer. Controversially, over-expression of 15-LOX-1 in HCT116 colon carcinoma cells has been stated to activate the ERK pathway and promote carcinogenesis, which was explained by the effect on redox state. However, 15-LOX-1 was also shown to be anti-tumorigenic in even the same cell line by pointing the reduction in the activity of NF-kB (Figure 1.6; Lee et al., 2011; Bhattacharya et al., 2009; Kuhn et al., 2015). 15-LOX-1 has been linked to regulated necrosis via regulation of intracellular redox state by cooperating with 12-LOX (Berghe et al., 2014).
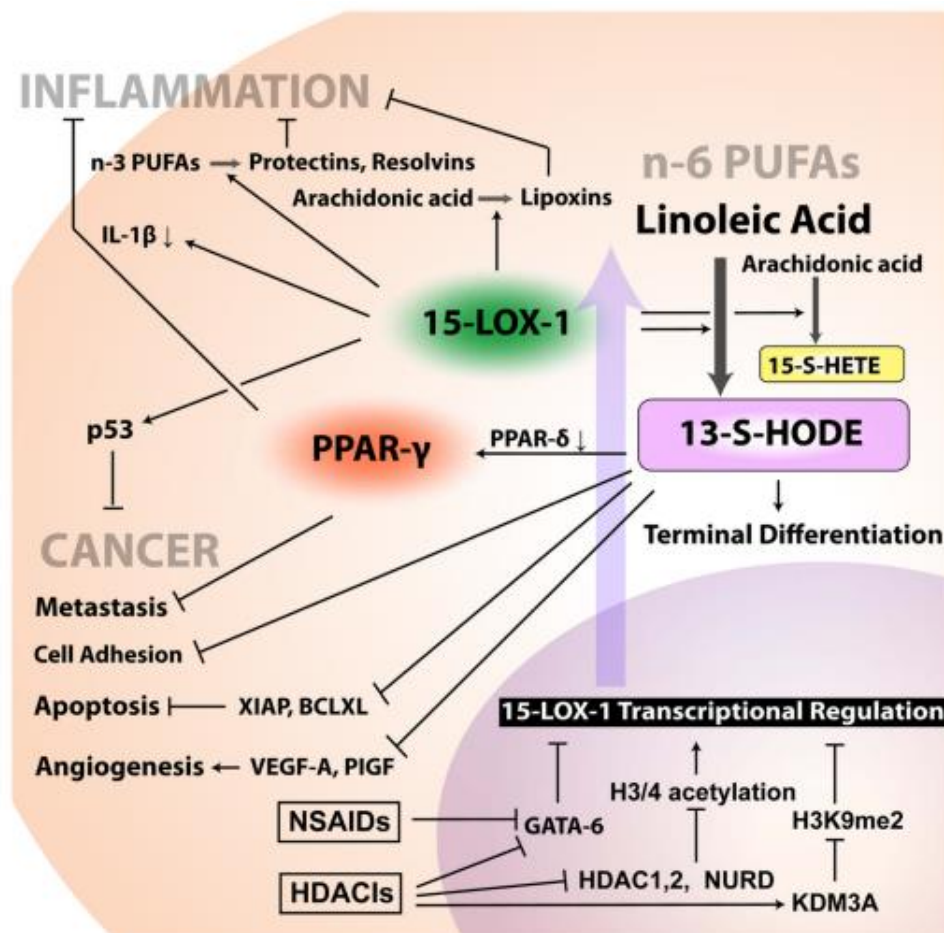
Figure 1-7 General mechanisms and transcriptional regulation of 15-LOX-1 in cancer and inflammation (Lee et al., 2011).

There have been limited number of studies on the association of 15-LOX-1 with cancer drug resistance, which was not enough to decipher the possible role of 15-LOX-1 in resistance to anti-cancer drugs. Chen et al. showed that the expression of 15-LOX-1 was increased in endogenously imatinib-resistant chronic myeloid leukemia stem cells when they were treated with imatinib (Chen et al., 2014). However, the study did not focus on the mechanisms behind these results.

1.5 Aim of the study

The present study aims to identify the possible role and the mechanisms of 15-LOX-1 in cancer drug resistance. To address this investigation,

- The expression status of 15-LOX-1 in different types of drug-resistant cells compared to their sensitive counterparts
- Effects of the upregulation/downregulation of the 15-LOX-1 on cell viabilities and drug sensitivity
- Molecular mechanisms of the 15-LOX-1-mediated alterations

were aimed to be examined.

CHAPTER 2

MATERIALS AND METHODS

2.1 Cell Lines and Cell Culture

Doxorubicin-sensitive human breast adenocarcinoma cell line, MCF7 and human cervical cancer cell line, HeLa, their resistant counterparts (MCF7 DOX and HeLa DOX), and zoledronic acid-resistant MCF7 cells (MCF7 ZOL) were used in the present study. Drug-resistant cell lines were developed previously in our laboratory by a stepwise increase in the drug concentrations (Kars et al., 2007; İşeri, 2009; Erdem, 2014). RPMI 1640 medium was used for cell culturing in the presence of 10% (v/v) heat-inactivated filter-sterilized FBS and 0.1% (v/v) gentamycin. To sustain the resistance phenotype, the doxorubicin-resistant cells and zoledronic acid-resistant cells were treated with 1 µM of doxorubicin and 8 µM of zoledronic acid, respectively. The resistance status was routinely checked by cell viability assays. A PCR-based method was used to check the Mycoplasma contamination (Young et al., 2010).

2.2 Sub-culturing

To obtain the proper cell stage (80% confluence) for any treatment or transfections and to sustain the cells for further studies, cells were routinely passaged in a T75 flask (Gibco, USA). Firstly, the duplication periods of the cells were determined using a specific number of cells cultured and followed by cell counting. After duplication periods of the cells were determined, the sub-culturing was performed according to these periods. For sub-culturing, medium in the T75 flasks were aspirated. Then adherent cells were washed with PBS twice. Next, 1.5 ml of Trypsin-

EDTA (Biological Industries, Israel) was applied onto cells and the cells were incubated for 5 min at 37°C to completely detach the cells from the flask surfaces. Then, 4.5 ml of the FBS-containing full medium was added into the cells in the Trypsin solution to stop the activity of the Trypsin. The appropriate amount of the cells were re-seeded into another T75 flask or 6- or 96-well plates for further experiments. The final volume in the T75 flasks was completed to 9 ml.

2.3 Cell freezing and thawing

The cells were frozen for long term storage using DMSO. Cells were obtained in the Trypsin-medium solution as given in the sub-culturing section. Then, the solution was centrifuged at 200 g for 6 min at room temperature. During the centrifugation process, a mixture of full medium and DMSO (1:10; DMSO: full medium) was prepared. Next, the supernatant after centrifugation was discarded and the cell pellet was re-suspended by DMSO-containing solution. Then, cells were taken into cryovials and stored at -20°C for 1 h. Next, the cells were stored at -80°C for 2-3 months and liquid nitrogen for longer periods.

For cell thawing to re-use the frozen cells, the cryovials were immediately incubated at 37°C until the cells were completely thawed. Next, the cells were mixed by 5 ml full medium and centrifuged at 200 g for 6 min at room temperature. Finally, the supernatants were discarded and the cell pellets were re-suspended with 4 ml of full medium and seeded into T25 flasks for 24 h. Next, the confluence of the cells was checked and the cells were taken into T75 flasks.

2.4 Cell counting by Trypan Blue cell exclusion method

Cells were routinely counted for obtaining a proliferation curve and seeding them for further experiments. Cells were collected in 15 ml falcon as given in the sub-culturing section and 90 µl of the cell suspension was mixed by 10 µl 0.5% Trypan

Blue solution. The mixture was incubated at room temperature for 2 min and then cells were loaded to a Neubauer hemacytometer (Brightline, Hausser Scientific, USA). Then, the stained cells, whether blue (death) or brownish (live) were counted using a phase-contrast microscope (Olympus, USA).

Cell number/ml was determined by using the formula given below:

Cell number/ml = Average cell count per square x Dilution factor x 4 x 106

2.5 Gene expression analysis

The expressions of the specific genes were followed by quantitative reverse transcriptase-polymerase chain reaction (qRT-PCR). The protocols to obtain complementary DNA (cDNA) and qRT-PCR were given below.

2.5.1 Isolation of total RNA

TRIzol reagent (Thermo Fisher Scientific, USA) was used for total RNA isolation. The manufacturer's instructions were followed during the isolation protocol. Cells were seeded into 6-well plates as 35×10^4 cells/wells and incubated for two days. Next, any treatments including transfections or drug administrations were performed for two days or cells incubated for three days in the absence of treatments. Cells were obtained as pellets by centrifugation at 200 g for 6 min at room temperature. Then, the cell pellets were washed by PBS twice. Next, the cell pellets were completely re-suspended by 1 ml of Trizol solution in a 1.5 ml Eppendorf tubes. 200 µl chloroform was added on to Tizol-cell mixture and incubated on ice for 15 min. Next, the mixture was centrifuged at 12000 g for 15 min at 4°C. The aqueous phase that contains RNAs was taken into another sterile Eppendorf tube after centrifugation. 1 ml of ice-cold isopropanol was added onto this phase and incubated for 10 min at room temperature. Next, the mixture was centrifuged at 12000 g for 15 min and supernatant was

carefully discarded. The pellet was washed with 70% ethanol and re-centrifuged at 12000 g for 10 min. Finally, the supernatant was discarded without disturbing the pellet and the pellet was let to dry for about 10 min at room temperature. The pellet was re-suspended in RNase free water. The concentration of the total RNA was determined by NanoDrop (BioDrop, UK) and OD260/280 and OD260/230 values were followed to be between 1.8-2.2 which gave the purity of the RNA samples. The RNA integrity was also checked by 2% agarose gel electrophoresis. RNA samples were stored at -80°C until they were used.

2.5.2 DNase treatment and cDNA synthesis

Possible DNA contamination after total RNA isolation was eliminated using DNase treatment. 1.5 µg of total RNA was mixed by 1 µl DNase (Thermo Fisher Scientific, USA) in the presence of 1 µl DNase buffer and nuclease-free water up to 10 µl final volume. The mixture was incubated at 37°C for 1 h and the enzyme was inhibited by 1 µl EDTA solution by incubating at 65°C for 10 min. Next, DNase-treated RNA samples were mixed by 1 µl of random hexamer and 0.5 µl nuclease-free water and incubated at 65°C for 5 min. Finally, a mixture of 4 µl reaction buffer, 2 µl ready-to-use dNTP mix, 0.5 µl RiboLock RNase inhibitor and 1 µl RevertAid Reverse Transcriptase was added onto the random hexamer-including mixture and incubated at 25°C for 10 min, 42°C for 1 h and 72°C for 10 min to synthesize cDNA. cDNA samples were stored at -20°C until they were used.

2.5.3 Quantitative Reverse Transcriptase Polymerase Chain Reaction (qRT-PCR)

Expressions of specific genes were analysed by qRT-PCR. The qRT-PCR procedures were carried out by SsoAdvanced Universal SYBR Green Supermix (BioRad Inc., USA) using BioRad CFX device. The primers used for qRT-PCR were listed at Table 2.1.

Table 0-1 Primer sequences used for gene expression studies.

Gene	Primer Type	Sequence
ALOX15	Forward	5' GCCTAAGGCTGTGCTGAAGA 3'
	Reverse	5' GGGCTATAACCACGAAGGGG 3'
PPARG	Forward	5' TGCGAAAGCCTTTTGGTGAC 3'
	Reverse	5' GGGCTTGTAGCAGGTTGTCT 3'
ACTB	Forward	5' CCAACCGCGAGAAGATGA 3'
	Reverse	5' CCAGAGGCGTACAGGGATAG 3'

During the gene expression studies, *ACTB* was used as a reference to perform relative expression of the genes. The ingredients and reaction conditions were given in Table 2.2. The thresholds were obtained using standard which were prepared from a sample as 1:2; 1:10; 1:50; 1:200 dilutions during the Ct determination process. All the cDNAs were diluted 10-fold before using as template in qRT-PCR.

Table 0-2 PCR ingredients and conditions for expressions of apoptosis-related genes

Ingredient	Concentration	Volume	Final Concentration
SsoAdvanced Universal SYBR Green Supermix	2X	5 µl	1X
Forward primer	5 µM	1 µl	0.25 µM
Reverse primer	5 µM	1 µl	0.25 µM
Template		3 µl	
Total		10 µl	

Initial denaturation	95°C	5 min	1 cycle
Denaturation	95°C	30 s	
Annealing	60°C	30 s	45 cycles
Extension	72°C	30 s	
Final elongation	72°C	10 min	1 cycle
Melting	55 – 99 °C		1 cycle

2.5.4 Quantification of qRT-PCR

qRT-PCR data were quantified by DDC$_t$ ($2^{\Delta\Delta Ct}$) method (Livak & Schmittgen, 2001). Fold changes in expression were calculated by the formula of $2^{-\Delta\Delta Ct}$ where ΔΔCt is calculated by the formula below:

ΔΔCt = ((Ct$_{Target}$)-(Ct$_{Reference}$)$_{Treated}$)-((Ct$_{Target}$)-(Ct$_{Reference}$)$_{Untreated}$)

2.6 Genetic manipulations

To reverse the expression status of 15-LOX-1 in the cell lines, a short hairpin RNA (shRNA) vector (pSUPER-shALOX15) was designed as the details were given below. The overexpression vector, pcDNA3.1(-)-ALOX15 was kindly provided by Prof. Sreeparna Banerjee.

2.6.1 Design of pSUPER-shALOX15 vector

To downregulate the 15-LOX-1 in drug-sensitive MCF7 and HeLa cells, an shRNA vector targeting *ALOX15* was designed in the presence of scrambled control according to the literature (Mumy et al., 2008) using pSUPER vector (Figure 2.1).
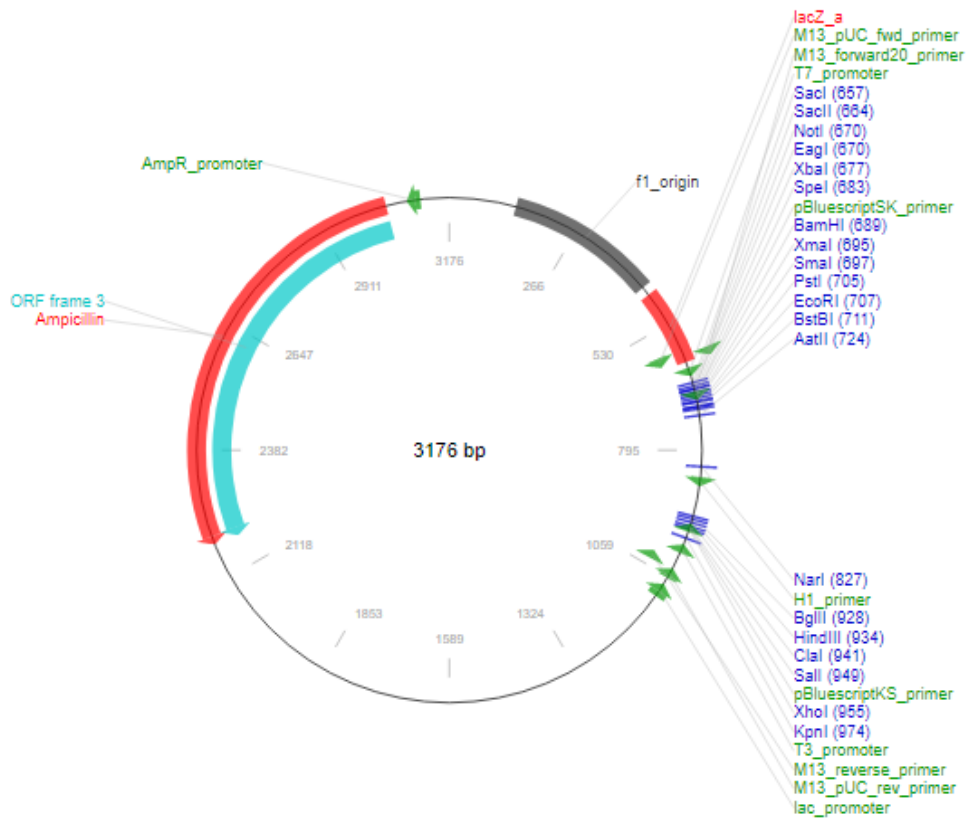
Figure 0-1 The backbone of pSUPER vector.

2.6.1.1 Insert preparation

The sequences of the sense and antisense *ALOX15*-targeting and scramble shRNA were given below.

ALOX15-shRNA-sense

GATCCCCTCGTGAGTCTCCACTATAATTCAAGAGATTATAGTGGAGACT CACGATTTTTGGAAA

ALOX15-shRNA-antisense

AGCTTTTCCAAAAATCGTGAGTCTCCACTATAATCTCTTGAATTATAGT GGAGACTCACGAGGG

24

Scrambled-shRNA-sense

GATCCCCCATCCTATCTTCAAGCTTATTCAAGAGATAAGCTTGAAGATA
GGATGTTTTTGGAAA

Scrambled-shRNA-antisense

AGCTTTTCCAAAAACATCCTATCTTCAAGCTTATCTCTTGAATAAGCTTG
AAGATAGGATGGGG

The sense and anti-sense sequences were ordered and dissolved to a final concentration of 1 µg by nuclease-free water. Next, the sense and anti-sense oligos were mixed at a ratio of 1:1 and incubated at 95ºC for 5 min on a dry heating block. Then, the device was turned off and the mixture was cooled to room temperature overnight. The annealing of the oligos were controlled by 3% agarose gel in the presence of sense- and anti-sense-alone controls. The annealed oligos contained the sequences of the enzymatic cute sites of *XhoI* and *HindIII* restriction enzymes which were used for the molecular cloning into pSUPER vector.

2.6.1.2 Double digestion

To clone the insert into pSUPER vector, the vector was cut with *XhoI* and *HidIII* (Thermo Scientific, USA) to create sticky ends. The vector was cut with these enzymes according to Table 2.3.

Table 0-3 Ingredients of digestion reaction.

pSUPER vector	25 µl
Tango Buffer	10 µl
BamHI	2 µl
XhoI	2 µl
Nuclease free water	11 µl
Total	50 µl

The digestion mixtures were incubated at 37°C for 2 h. After the incubation period, the digested vector was run on 0.8% agarose gel at 100 V for 30 min. Then, the digested the vector were extracted from agarose gel.

2.6.1.3 Gel Extraction

The double digested vector was extracted from agarose gel using Zymoclean Gel DNA Recovery Kit (Zymo Research, USA). Briefly, DNA was excised from the gel with a sterile blade and taken into a sterile 1.5 ml Eppendorf tube. Then, 1 ml of ADB Buffer was added on the gel and the gel slice was incubated at 55°C for 10 min until the gel was completely dissolved. Then, the solution was taken into a Zymo-Spin column and centrifuged at 12000 g for 2 min and the flow-through was discarded. DNA on filter was washed twice by 200 µl DNA Wash buffer by centrifugation at 12000 g for 1 min. Next, the filter was centrifuged again at 12000 g for 1 min to remove possible residual alcohol. 10 µl of DNA elution buffer was added directly to the filter and incubated at room temperature for 1 min and centrifuged at 12000 g for 1 min. The concentration of the DNA was determined by NanoDrop.

2.6.1.4 Ligation

To ligate the insert and the vector with sticky ends, T4 DNA Ligase (Thermo Fisher Scientific, USA) was used. Briefly, 50 ng vector was mixed with the insert at a ratio 1:9. The ingredients and amounts of ligation reaction were given below.

Table 0-4 Ingredients of ligation reaction.

Ingredients	Volume
T4 DNA Ligase buffer	1 µl
Vector	1 µl
Insert	5 µl
T4 DNA Ligase	1.5 µl
Nuclease free water	1.5 µl
Total	10 µl

The mixture was incubated at 25°C for 4 h to ligate the sticky ends and form a circular plasmid. The ligated plasmid (pSUPER-shALOX15) was transformed into competent *E. coli* cells as described below.

2.6.1.5 Colony PCR

The success of insertion of *ALOX15* and scramble shRNAs was controlled by colony PCR using the universal primers of CMV forward primer and BGH reverse primer whose complementary sites were located on the pSUPER vector. The PCR ingredients and conditions were shown in Table 2.5.

Table 0-5 Ingredients and conditions of colony PCR.

Ingredients	Concentration	Volume
Taq buffer	10X	2.5 μl
MgCl$_2$		2 μl
dNTP mix	10 mM each	0.5 μl
Forward primer	25 μM	0.5 μl
Reverse primer	25 μM	0.5 μl
Taq polymerase		0.2 μl
Template		2.5 μl
PCR grade water		16.3 μl
Total		25 μl

Pre-incubation	94°C	5 min	1 cycle
Denaturation	94°C	30 s	
Annealing	60°C	30 s	35 cycles
Elongation	72°C	1 min	
Final elongation	72°C	10 min	1 cycle

PCR products were run on 1% (w/v) agarose gel at 100 V for 30 min. The colonies showing correct bands (at ~550 bp) was taken into LB and grown at 37°C with shaking at 200 rpm. The insert-containing plasmids were isolated by Plasmid Isolation kit (Zymo Research, USA) as described below.

2.7 Competent *E. coli* preparation

XL1 Blue *E. coli* cells were streaked on LB agar and grown at 37°C by shaking at 250 rpm overnight. Next, single colonies were selected and inoculated into 10 ml of LB media, and incubated at 37°C overnight. 5 ml cell suspension was inoculated into 100 ml of LB media and OD was followed to be 0.4. Then, the cells were incubated on ice for 20 min and centrifuged at 3000 rpm for 3 min at 4°C. The supernatants were discarded and the pellets were dissolved in 30 ml cold 0.1 M $CaCl_2$ solution for 30 min. Finally, the cells were centrifuged at 3000 rpm for 3 min at 4°C and the cell pellets were dissolved in cold 0.1M $CaCl_2$ in 15% glycerol solution as 100 µl of aliquots in sterile tubes and immediately transferred into liquid nitrogen and stored at -80°C until they were used.

2.8 Transformation

Competent cells were treated with 1 ng of the pcDNA3.1(-)-ALOX15 or the total volume of ligation reaction for pSUPER-shALOX15. The cells were incubated on ice for 1 h. Next, the cells were heat-shocked at 42 °C for 45 min and incubated on ice for 2 extra min. Then, 750 µl LB was added onto the heat-shocked cells and incubated at 37 °C for 1 h by shaking at 250 rpm. Finally, the cells were pelleted by centrifugation at 3000 rpm for 3 min and the pellet was streaked into Ampicillin-containing LB agar plates. The plates were incubated at 37°C overnight. Then, the single cells were inoculated into 4 ml of Ampicillin-containing LB media and incubated at 37°C overnight by shaking at 250 rpm. Finally, the suspension was used for plasmid isolation.

2.9 Plasmid isolation

The plasmid isolation was performed by MiniPrep Plasmid Isolation Kit (Zymo Research, USA) according to the manufacturer's instructions. Briefly, 100 µl of 7X

lysis buffer was added onto 600 µl of transformed *E. coli* cells, and the mixture was incubated at room temperature for 2 min. Next, this solution was mixed by 350 µl cold neutralization buffer and the colour change from blue to yellow was followed. The mixture was centrifuged at 14000 g for 6 min to pellet the cell debris. The supernatant was taken into Zymo-Spin IIN column and centrifuged at 14000 g for 1 min to bind the plasmids on the filter. The filters were washed by 200 µl Endo-Wash buffer and 400 µl Zyppy Wash buffer by centrifugation at 14000 g for 1 min and 30 sec, respectively. Then, the filter was centriguged at full speed for 1 min to eliminate the alcohol and taken into a sterile 1.5-ml Eppendorf tube. Finally, 32 µl Zyppy Elution buffer was added directly onto the filter and isolated plasmids were obtained by centrifugation at 14000 rpm for 1 min. The concentrations of the plasmids were determined by BioDrop spectrophotometer (BioDrop, UK).

2.10 Transfection of cells

A previously designed overexpression vector, pcDNA3.1(-)-ALOX15 (Cimen et al., 2009) was used to overexpress the 15-LOX-1 in paternal MCF7 and doxorubicin-resistant MCF7 and HeLa cell lines. $3x10^5$ cells/wells and $1x10^4$ cells/well were seeded into 6-well plates and 96-well plates, respectively. The cells were incubated for 48 h and transient transfections were performed by Turbofect transfection reagent (Thermo Scientific, USA) using 1.5 µg plasmid for 6-well plate and 72.5 ng for 96-well plate for 48 h. Then, RNA or DNA isolations were performed using 6-well plate and cell viability assay was carried out using 96-well plate. All transfections were carried out in the presence of un-transfected (UT) control and empty vector (EV) control.

2.11 Western Blotting

2.11.1 Total protein isolation and determination of protein concentration

Total protein was isolated from treated or untreated cells using RIPA Lysis and Extraction Buffer (Thermo Fisher Scientific, USA). The cells were harvested by centrifugation and lysed in 1 ml of cold RIPA buffer containing 100X Halt Protease and Phosphatase Inhibitor cocktails (Thermo Fisher Scientific, USA) for 30 min on ice by vortexing in regular intervals. Then, lysed samples were centrifuged for 30 min at 14000 g to remove the cell debris. Protein containing supernatant was taken to a sterile Eppendorf tube. Protein concentration was determined by Coomassie (Bradford) Protein Assay Kit (Thermo Scientific, USA).

2.11.2 Sodium Dodecyl Sulphate-Polyacrylamid Gel Electrophoresis (SDS-PAGE)

To separate the proteins, isolated protein samples were firstly run on sodium dodecyl sulphate-polyacrylamid gels in Mini-PROTEAN Tetra Cell gel system (Bio-Rad Laboratories, USA). For that aim, 12% separating gel mixture was prepared and loaded between the glass sandwich system. The surface of the mixture was covered with isopropanol to prevent inhibition of gel polymerization and provide a smooth gel surface. After polymerization, 5% stacking gel mixture was prepared and loaded on separating gel. Comb was placed and the gel mixture was allowed to polymerize. The ingredients and concentrations of separating and stacking gels were given in Table 2.6.

Table 0-6 Ingredients and amounts of stacking and separating gels.

Ingredient	5% stacking gel	8% separating gel
30% acrylamide-bisacrylamide solution (37:5:1)	850 µl	2.7 ml
1M Tris buffer (pH 6.8)	625 µl	----
1.5M Tris buffer (pH 8.8)	----	2.5 ml
10% APS	50 µl	100 µl
10% SDS	50 µl	100 µl
TEMED	5 µl	5 µl
dH$_2$O	3.4 ml	4.6 ml
Total	5 ml	10 ml

50 µg of protein solution was mixed with 6X protein loading buffer which contains β-mercaptoethanol and incubated at 95°C for 5 min to completely denature proteins. The denatured protein samples were vortexed briefly and centrifuged, loaded on previously casted polyacrylamide gel with pre-stained protein marker (Thermo Fisher Scientific, USA) and run at 100V in stacking and 150V in separating gel for approximately 45 min.

2.11.3 Wet transfer

To transfer the proteins on the gel to the membrane, the gel, pre-cut nitrocellulose membrane and filter papers, which will be used in wet transfer process, were incubated in cold transfer buffer for 15 min. Next, a sandwich system containing filter papers, membrane and gel were prepared in the transfer system. The gel on the membrane localization was scanned carefully to remove any air bubbles. The sandwich was placed in the gel tank with an ice box on a magnetic stirrer. Finally,

the tank was filled with cold transfer buffer and transfer was carried out at 25 V at 4°C for 1 h.

2.11.4 Membrane blocking

To minimize the non-specific binding of the primary antibodies to the membrane, the membrane was blocked by 5% BSA (w/v) in 0.1% TBST buffer (1X TBS buffer containing 0.1% v/v Tween20) for 1 h at room temperature by gently shaking on a shaker.

2.11.5 Western Blotting and imaging

After the blocking process, the membranes were probed with a mouse anti-15-LOX-1 (1:1000; Abnova, Taiwan) or a mouse anti-active caspase 3 antibody (1:1000; Bioss Antibodies Inc., USA) or anti-Beta-actin antibody (1:1000; Abcam, USA) as loading control at 4°C overnight. Next, the membranes were washed three times by 0.05% TBST solution and incubated with HRP-conjugated goat anti-mouse antibody (1:2000; Abcam, USA). Then, the membranes were again washed three times by 0.05% TBST solution and protein bands were visualized using the ECL kit (Thermo Scientific, USA) according to the manufacturer's instructions using ChemiDoc XRS+ system (BioRad, USA).

2.12 Actinomycin D treatment

The check the mRNA stability, doxorubicin-sensitive and -resistant MCF7 cells were seeded into 6-well plate. Cells were treated with 10 µg/ml of Actinomycin D (10 mg/ml; Tocris Bioscience, USA) and incubated for 2, 4 or 6 h in the presence of untreated control. Next, total RNAs were isolated by method explained above and the relative expressions of *ALOX15* were determined by qRT-PCR as detailed above.

2.13 Fatty acid methyl ester (FAME) profiling

GC/MS method was used to determine FAME profiles of the cells. Firstly, Bligh-Dyer method (Bligh and Dyer, 1959) was used to isolate total lipids. During this method, cells were treated with chloroform/methanol solution (1:2) in 1 ml PBS in glass tubes, and vortexed rigorously for 2 min. Next, chloroform was added onto mixture and vortexed for 30 sec. Finally, 1.5 M NaCl was added onto the mixture and vortexed for 30 seconds, and centrifuged at 500 g for 10 min. The liquid phase of total lipids was evaporated under N_2 to prevent oxidation. Next, 0.1 gram of total lipid sample was dissolved in 0.5 ml of 2 M potassium hydroxide (prepared in methanol) and mixed well. 10 ml of hexane was added to the mixture, and centrifuged for 15 min at 5000 rpm and 20^0C. The upper (liquid) phase was used for the GC/MS analysis. The analysis of FAMEs was performed using Shimadzu GC-2010 plus, equipped with Shimadzu GCMS-QP2020 mass spectrometer (Shimadzu Corporation, Japan) and Restek Rt-2560 capillary column (100 m, 0.25 mm ID, 0.20 µm; Restek, USA). An electron ionization system with ionization energy of 70 eV was used for GC-MS detection. Helium at a flow rate of 1 ml/min was used as the carrier gas. Injector and ion source temperatures were set at 250^0C and 200^0C, respectively. The column temperature was initially at 40^0C, then gradually increased to 140^0C and held for 5 min, and finally increased to 240^0C. Samples at 1 ml volume were subjected to split injection using Shimadzu AOC-20s auto sampler and AOC-20i auto injector. The fatty acid components of samples were identified by comparing retention time and mass spectra with those of methyl ester standards. The relative amount of each fatty acid was quantitatively expressed as percent of total fatty acids by integrating the area under the individual peak and dividing the result by the total area for all fatty acids (Rise et al., 2007). The GC/MS results were obtained via service of Konya Food and Agriculture University, Konya, Turkey.

2.14 Cell viability assay

The cell viabilities were determined by 3-(4,5-dimethylthiazol-2-yl)-2,5 diphenyltetrazolium bromide (MTT) assay. Cells were transfected with pcDNA3.1(-)-15-LOX-1 or empty vector to see the effects of transfection, treated with drugs to see the effects of drug treatment or firstly transfected and then treated with drugs to see the effect of the combination on cell viabilities for definite time periods. Then, 10 µl of MTT solution (5 mg/ml) was added onto cells and incubated for 4 h. Next, cells were disrupted by SDS-HCl solution (1 g SDS in 0.01 M HCl in 10 ml final volume) and incubated at 37°C overnight in the incubator. The ODs were read at 570 nm by a microplate spectrophotometer (Multiskan GO; Thermo Fisher Scientific, USA). The viability of untreated control group was accepted as 100% and the relative cell viability of treated cells was determined accordingly. The IC_{50} values were determined by nonlinear regression tests using GraphPad Prism 8.0 software (GraphPad Inc.).

2.15 Intracellular drug accumulation assay

The accumulation of doxorubicin in transfected MCF7 DOX and HeLa DOX cells were followed by the fluorescent nature of the doxorubicin under a fluorescence microscope. The cells were transfected with pcDNA3.1(-)-ALOX15 plasmid or empty vector for 48 h. Next, the cells were treated with 10 µM doxorubicin for 4 h and CellTracker™ Blue CMAC (Thermo Scientific, USA) according to the manufacturer's protocol. Then, cells were fixed with cold ethanol followed by mounting of the coverslips on slides. Images were obtained with a Leica DM3000 LED confocal microscope (Leica Microsystems, Germany).

2.16 15-LOX-1 activity assay

13(S)-HODE amounts were detected for 15-LOX-1 activity analyses by the 13(S)-HODE ELISA Kit (Abcam, USA). Total lipids were isolated by Bligh-Dyer method as described above and the ELISA protocol was applied according to the supplier's protocol. Briefly, reagents, standards and plate templates were prepared according to the kit's instructions. All reagents were warmed to room temperature. 100 μl of appropriate diluent was added into proper wells. Next, 50 μl of 13(S)-HODE Alkaline Phosphatase Conjugate was added onto the solutions. Then, 50 μl 13(S)-HODE antibody was added into the appropriate wells. The plates were incubated at room temperature for 2 h by shaking at 500 rpm after the plates were sealed. The solutions were discarded and wells were washed by 1X Wash Buffer three times. 5 μl 13(S)-HODE Alkaline Phosphatase Conjugate 1:10 dilution was added into the wells. Next, 200 μl pNpp Substrate was added onto the samples and the plates were incubated at 37°C for 2 h. Finally, 50 μl Stop Solution was added into wells and ODs were obtained at 405 nm in the presence of 590 nm correction OD by an ELISA reader.

2.17 Apoptosis assay

To assess the apoptosis, Caspase 3/7 activity was determined by Apo-ONE® Homogeneous Caspase 3/7 Assay (Promega, USA). The cells were transfected with pcDNA3.1(-)-ALOX15 or empty vector in the presence of untreated and Etoposide-treated control groups. Next, Caspase 3/7 activity was followed according to the supplier's instructions. Briefly, Apo-ONE® Caspase Reagent was prepared by mixing caspase substrate with reaction buffer (1:100) and added to each well with 1:1 ratio in black 96-well plates. The blanks were set as only medium and caspase reagent containing wells. The fluorescent signal was measured at 521 nm by using SpectraMax iD3 Multi-Mode Microplate Reader (Molecular Devices, USA).

2.18 Cell motility assay

Cell motilities were followed by an *in vitro* wound-healing assay. Cells were seeded into the 6-well plates and transfected with the pcDNA3.1(-)-ALOX15 expression vector in the presence of empty vector control for 48 h. Next, an area was denuded by a pipet tip and cells were imaged at day 0, 1, 2, 3 and 4 under a light microscope. The cells were washed with PBS to remove debris and the medium was changed prior to photography. The lengths of the wounds were determined by ImageJ Software (Schneider et al., 2012).

2.19 Cell cycle analyses

Flow cytometry was used for the determination of cell cycle distributions. Cells were transfected with pcDNA3.1(-)-ALOX15 or empty vector for 48 h. Next, the cells were washed PBS for three times, trypsinized and centrifuged to collect as pellets. The cells were fixed overnight by 80% ethanol at -20°C and washed twice with PBS after fixation. Then, the cells were incubated with 0.5 ml of PBS containing 100 μg/ml RNase (Thermo Scientific, USA) and 50 μg/ml propidium iodide (Sigma Aldrich, USA) at 37°C for 30 min. Cell cycle distribution was analysed by measuring DNA content using a flow cytometer (BD Accuri C6, BD Biosciences, USA). Data were analysed in triplicate using the BD Accuri C6 Software.

2.20 Chromosomal microarray (CMA)

Genomic DNAs of doxorubicin-sensitive and –resistant MCF7 and HeLa cells were isolated by spin columns (Zymo Research, USA) and the quality of isolated DNAs was evaluated by agarose gel electrophoresis. CMA was performed using Agilent 8×60K chips (Santa Clara, CA, USA), according to the manufacturer's instructions, to study copy number variations. Agilent Cytogenomics software was used for analyses. Data were presented as minimum coordinates (sequence positions of the

first and last probes within the CNV) in the NCBI37/hg19 genome assembly. The significant alterations in CMA analyses were determined using an in-house database of the Department of Medical Genetics, Faculty of Medicine, Gazi University, Ankara, Turkey. The log ratio that was given by the internal calculation of the system is a marker of the copy number of the genes and is calculated by $Log_2(Sample/Reference)$ where if the number of the gene equals to 2 as in the reference, then the log ratio will be zero; if the number of the gene equals to 3, then the log ratio will be 0.6; and if the number of the gene equals to 1, then the log ratio will be -1 (CytoGenomics 3.0, Agilent Technologies, USA).

2.21 Statistical analysis

All experiments were performed as three independent experimental set, each of which containing triplicates. Data were represented as mean ± SEM and analysed with t-test or one-way ANOVA test followed by post-hoc Tukey's test. Results were accepted as significant when $p < 0.05$.

CHAPTER 3

RESULTS AND DISCUSSION

The present study aims to investigate the possible role of 15-LOX-1 in cancer drug resistance by focussing on especially doxorubicin resistance in human breast adenocarcinoma cell line, MCF7 and human cervical cancer cell line, HeLa. Up to this study and its published form (Kazan et al., 2019), 15-LOX-1 has not been linked to cancer drug resistance in details. In this section, the results were presented in the frame of published article (Kazan et al., 2019).

3.1 Expression of 15-LOX-1 in the drug-sensitive and doxorubicin-resistant cells

To address the possible link between cancer drug resistance and 15-LOX-1 function, the expression profiles of 15-LOX-1 was determined in doxorubicin-resistant MCF7 (MCF7 DOX) and HeLa (HeLa DOX) cells in the presence of drug-sensitive parental cell lines. The resistance status were previously determined by determining the IC50 values for resistant and sensitive cell lines (Kars et al., 2006). All cell lines were checked for doxorubicin resistance to ensure the resistance status of the cell lines.

The expression of 15-LOX-1 was determined at mRNA level by qRT-PCR in MCF7 DOX and HeLa DOX cells compared to their sensitive counterparts. The results showed that 15-LOX-1 was downregulated in doxorubicin-resistant MCF7 and HeLa cells (Figure 3.1A and B).
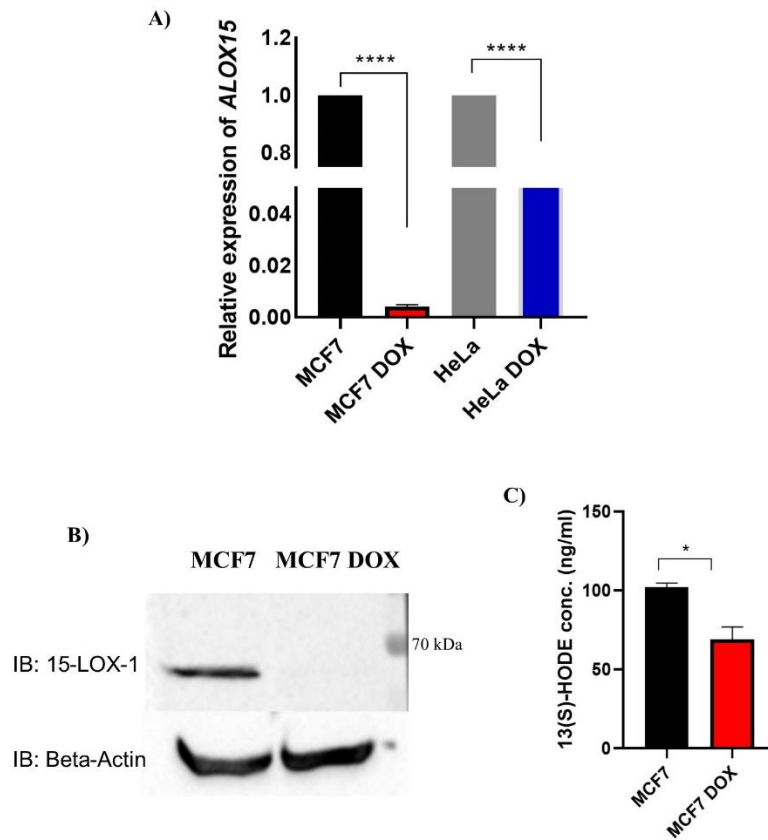
Figure 0-1 Expression and activity of 15-LOX-1 in resistant cell lines compared to their sensitive counterparts. A) Expression of *ALOX15* was determined by qRT-PCR in MCF7 DOX and HeLa DOX cells compared to MCF7 and HeLa cells, respectively. B) 15-LOX-1 expression was determined at protein level in MCF7 and MCF7 DOX cells by Western Blotting method. C) 13(S)-HODE amount was assessed to determine the activity of the 15-LOX-1 in MCF7 and MCF7 DOX cells. Data were analysed with t-test (*$p < 0.05$; ****$p < 0.0001$).

The downregulation of 15-LOX-1 at both mRNA and protein levels were shown for MCF7 DOX cells. However, although the downregulation of ALOX15 was shown in mRNA levels with the Ct values more than 30 in qRT-PCR for HeLa and HeLa DOX, the expression of 15-LOX-1 could not be detected at protein level even for HeLa cells. The reasons would be the translation limitations, pointing possible post-

transcriptional or translational modifications in these cell lines (Ostareck-Lederer et al., 1994; Ostareck et al., 1997).

To see whether the expression profile of 15-LOX-1 correlated with its function, the activity of 15-LOX-1 was demonstrated by detection of 13(S)-HODE amount in MCF7 DOX and MCF7 cells. As a specific product of the 15-LOX-1, 13(S)-HODE amounts were previously shown to be correlated by the enzyme activity (Cimen et al., 2009). The results underlined that the activity of 15-LOX-1 in addition to its expression was limited in MCF7 DOX cells compared to parental cells (Figure 3.1C).

Chen et al. showed that the expression of 15-LOX-1 was increased in endogenously imatinib-resistant chronic myeloid leukaemia stem cells contrary to the findings of the present study (Chen et al., 2014). Nevertheless, this difference could be a result of diverse tumour origin and the mechanism how the cells become resistant to the cells.

3.2 Expression of 15-LOX-1 in Zoledronic acid-resistant MCF7 cells

The study conducted by Chen et al. (2014) and the preliminary data of the present study implicated that the expression of the 15-LOX-1 could be cell and/or drug specific. Zoledronic resistant MCF7 cells (MCF7 ZOL) which was previously developed by stepwise increase in the drug concentration in our laboratory (Kars et al., 2007) was used to address this question. The results showed that 15-LOX-1 was not downregulated in MCF7 ZOL cells compared to MCF7 parental cells. These results revealed that the role of 15-LOX-1 in cancer drug resistance could be cell and/or drug specific.
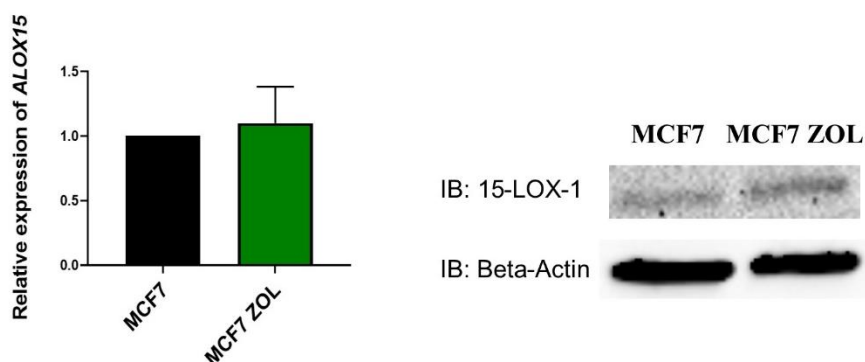
Figure 0-2 Expression of 15-LOX-1 in different drug-resistant cell lines. 15-LOX-1 expression was also determined for another drug (Zoledronic acid)-resistant MCF7 cells (MCF7 ZOL) in the presence of sensitive control at mRNA and protein levels. Data were analysed by t-test.

3.3 Regulation of ALOX15 expression

The molecular studies on cancer drug resistance generally assumed that the expression of a gene of interest was downregulated in a transcriptional regulation manner (Kudoh et al., 2000; Iseri et al., 2010; Kars et al., 2011; Urfali-Mamatoglu et al., 2018). Nonetheless, any downregulation or upregulation could be a result of copy number alterations in the gene.

In the frame of the hypothesis that any copy number variants (CNVs) could affect the expression of the 15-LOX-1, all chromosomes were scanned by chromosomal microarray method. The results showed that there were not any CNVs in the *ALOX15* gene (Figure 3.3 and 3.4). The mean logarithmic (log) ratios that were the indicator of the copy number of the gene were -0.37, 0.29, -0.07 and -0.24 for MCF7, MCF7 DOX, HeLa and HeLa DOX, respectively, which shows lack of a CNV. The *PPARG* gene was also scanned as the PPARγ is the last member of the 15-LOX-1-mediated reaction by binding 13(S)-HODE to show trigger cellular alterations (Cimen, et al., 2011; Tian et al., 2017). CNV analyses of the *PPARG* gene indicated that there were not any changes in the copy number of the *PPARG* gene in all cell lines with the log

42

ratios of 0.32, 0.56, 0.27 and 0.35 for MCF7, MCF7 DOX, HeLa and HeLa DOX, respectively.

Importantly, the copy number of *ABCB1* was also scanned during the CNV analyses. The results underlined that there were more than two copies of *ABCB1* in doxorubicin-resistant MCF7 and HeLa cells while the number of the gene was conserved in sensitive cells. The mean log ratios were 0.21 for MCF7 and 5.01 for MCF7 DOX where there were at least seven copies of the gene, and 0.30 for HeLa and 1.08 for HeLa DOX where there were three copies of the gene. The CNVs in doxorubicin-resistant cells were previously reported by Yamamoto et al. (2011). The researchers showed that the expression and also the copy number of the *ABCB1* were increased in this cell line. However, there have been not any studies reporting the CNV status of the *ABCB1* in doxorubicin-resistant HeLa cells. Thus, the present study is the first reporting showing the doxorubicin resistance in HeLa cells could be a result of CNVs in the *ABCB1* gene.
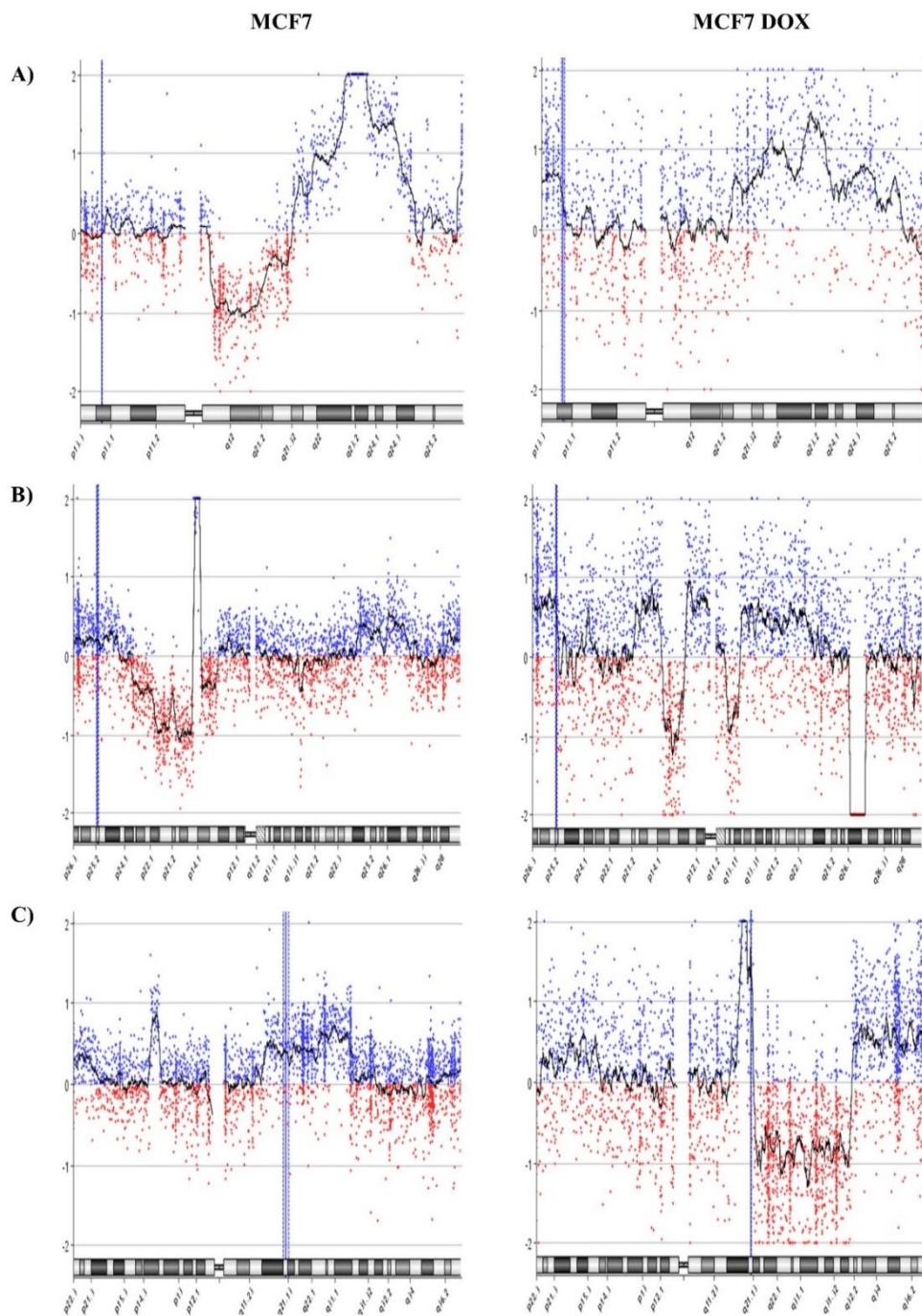
Figure 0-3 Copy number variations of A) *ALOX15* on chromosome 17, B) *PPARG* on chromosome 11 and C) *ABCB1* on chromosome 7 in MCF7 and MCF7 DOX cells. Blue lines indicate the localization of the gene of interest on the corresponding chromosome.
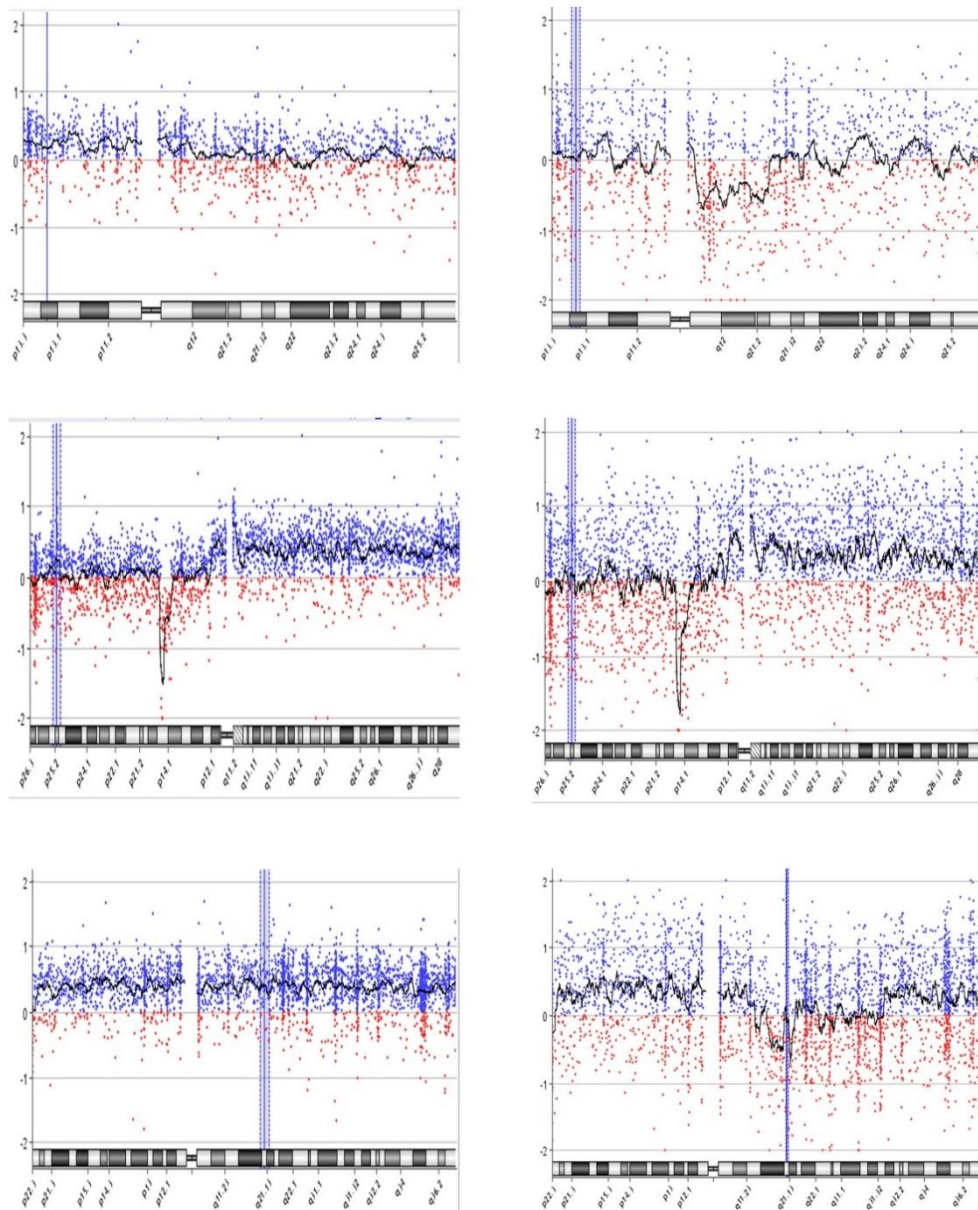
Figure 0-4 Copy number variations of A) *ALOX15* on chromosome 17, B) *PPARG* on chromosome 11 and C) *ABCB1* on chromosome 7 in HeLa and HeLa DOX cells. Blue lines indicate the localization of the gene of interest on the corresponding chromosome.

45

To totally explore the downregulation mechanism of *ALOX15* in MCF7 DOX cells, the cells were treated with Actinomycin D to stop the transcription and evaluate the mRNA stability in the presence of MCF7 sensitive control. The results illustrated that the mRNA of the *ALOX15* was less stable in MCF7 DOX cells while that in MCF7 cells was highly stable even for long term periods (Figure 3.5). These results underlined that the *ALOX15* was post-transcriptionally regulated in doxorubicin-resistant cell lines.
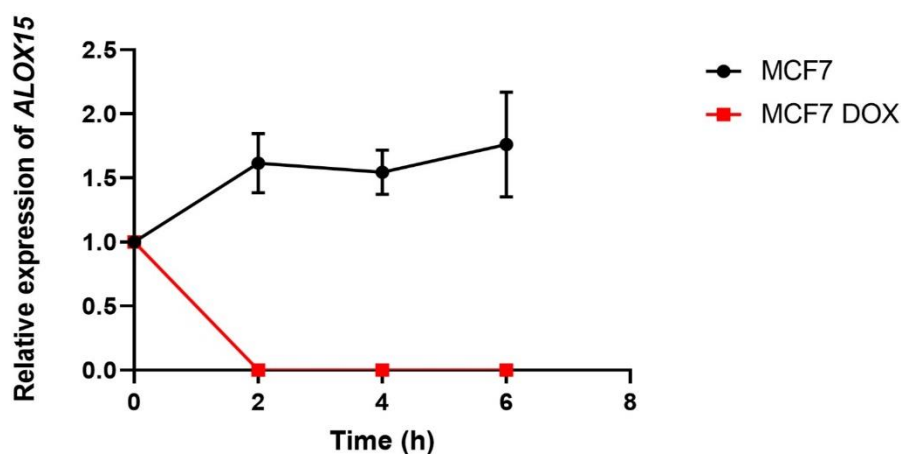
Figure 0-5 mRNA stabilities of *ALOX15* in MCF7 and MCF7 DOX cells. The stability of *ALOX15* mRNA was defined by Actinomycin D treatment at different time points for MCF7 and MCF7 DOX cells.

The expression of 15-LOX-1 is highly regulated at both transcriptional and post-transcriptional stages (O'Prey and Harrison, 1995). The transcription of 15-LOX-1 is controlled by IL-4 and γ-interferon in monocytes (Conrad et al., 1992); by bleeding, cholesterol feeding and phenylhydrazine (Bailey et al., 1995); by repressor proteins which bind to the differentiation control element (DICE) within the 3'UTR of the gene during erythroid differentiation (Ostareck-Lederer et al., 1994); by hnRNP proteins E1 and K for the regulation of the cytoplasmic translation (Ostareck et al., 1997; Thiele et al., 1999); by GATA6 as a transcriptional repressor (Shureiqi et al., 2007); and by histone deacetylase inhibitors (Tavakoli-Yaraki et al., 2013). Thus, any changes in those regulator regarding to the drug resistance mechanism

could affect the transcriptional or post-transcriptional regulation of 15-LOX-1 in doxorubicin-resistant cell lines.

3.4 Amounts of 15-LOX-1 substrates in sensitive and resistant cells

The main function of the 15-LOX-1 is to metabolize the polyunsaturated fatty acids (Tian et al., 2017). Hence, fatty acid profiles of the drug-resistant cells compared to their sensitive counterparts are critical in terms of assessing the function of the enzyme. Thus, the fatty acid profiling of the drug-sensitive and resistant cells were determined by GC/MS method (Table 3.1). The results figured out that there were not any significant differences between MCF7 and MCF7 DOX cells. Although caproic acid per cent slightly deviated in HeLa DOX cells compared to HeLa cells, the per cents of other lipids did not significantly deviate between the cell lines, pointing the fatty acid profiles were not different between doxorubicin-sensitive and resistant cell lines.

As the fatty acid profiles were similar between doxorubicin-sensitive and resistant cell lines, any alterations upon genetic manipulations of 15-LOX-1 levels were regarded as a result of protein itself but not that of substrate differences. Still, fatty acid profiles after 15-LOX-1 manipulation could be followed to see the effect of the protein on the substrate amount as a separate and further study in cancer drug resistance.

Table 0-1 Profiling of fatty acids in doxorubicin-sensitive and -resistant MCF7 and HeLa cells.

Fatty Acids	MCF7 (% ± SD)[†]	MCF7 DOX (% ± SD)	HeLa (% ± SD)	HeLa DOX (% ± SD)
Caproic acid (C6:0)	0.45 ± 0.21	0.17 ± 0.18	0.38 ± 0.006	0.28 ± 0.02*
Caprylic acid (C8:0)	2.84 ± 0.02	1.80 ± 0.93	2.30 ± 0.03	3.42 ± 2.005
Undecanoic acid (C11:0)	0.61 ± 0.45	0.35 ± 0.05	0.75 ± 0.07	1.29 ± 0.58
Myristic acid (C14:0)	0.29 ± 0.15	0.83 ± 0.58	0.40 ± 0.22	0.55 ± 0.02
Palmitic acid (C16:0)	17.51 ± 3.45	16.67 ± 5.98	22.42 ± 1.90	22.01 ± 1.09
Palmitoleic acid (C16:1)	1.53 ± 0.66	2.04 ± 2.26	0.88 ± 0.02	0.81 ± 0.01
Stearic acid (C18:0)	10.46 ± 1.14	9.81 ± 0.43	10.35 ± 0.95	10.46 ± 0.48
Oleic acid (C18:1n9c)	51.50 ± 3.42	46.05 ± 7.24	50.61 ± 4.41	48.46 ± 1.33
Linoleic acid (C18:2n6c)	1.04 ± 0.74	1.65 ± 1.12	1.10 ± 0.30	0.72 ± 0.16
Arachidic acid (C20:0)	1.10 ± 0.40	0.76 ± 0.60	1.02 ± 0.06	0.98 ± 0.74
Cis-11-eicosenoic acid (C20:1)	0.77 ± 0.49	0.97 ± 0.05	1.06 ± 1.12	1.27 ± 0.22
Cis-11,14-eicosadienoic acid (C20:2)	0.61 ± 0.08	0.62 ± 0.43	0.91 ± 0.17	0.63 ± 0.20
Behenic acid (C22:0)	1.12 ± 0.37	1.33 ± 0.17	1.48 ± 0.05	1.11 ± 0.30
Nervonic aid (C24:1)	0.96 ± 0.84	0.32 ± 0.27	0.91 ± 0.67	0.33 ± 0.27

[†] Data were presented as per cent of related lipids in total lipid moieties (100%) and analysed with t-test. *$p < 0.05$.

3.5 Overexpression of 15-LOX-1 in doxorubicin-resistant cells

To manipulate the expression levels of 15-LOX-1 in 15-LOX-1-downregulated MCF7 DOX and HeLa DOX cells to check the effects of replacement of the protein, a mammalian overexpression vector, pcDNA3.1(-)-ALOX15 was used. This vector was previously designed and the activity of the protein encoded by this vector was proved by laboratory group of Prof. Banerjee (Department of Biological Sciences, METU, Ankara; Cimen et al., 2009; Tuncer et al., 2017). The vector was transiently transferred to MCF7 DOX and HeLa DOX cells as explained in the materials and methods section. The efficacy of the transfection process and the availability of the protein was assessed by qRT-PCR and Western Blotting. The vector backbone that did not include *ALOX15* cDNA was used as empty vector (EV) control.

The overexpression studies showed that the expression of 15-LOX-1 was significantly elevated in MCF7 DOX and HeLa DOX cells when compared to untreated and EV controls at mRNA and protein levels (Figure 3.7). These results underlined that any alterations in cellular context will be a result of overexpression of 15-LOX-1 in those cell lines compared to untreated and EV controls.
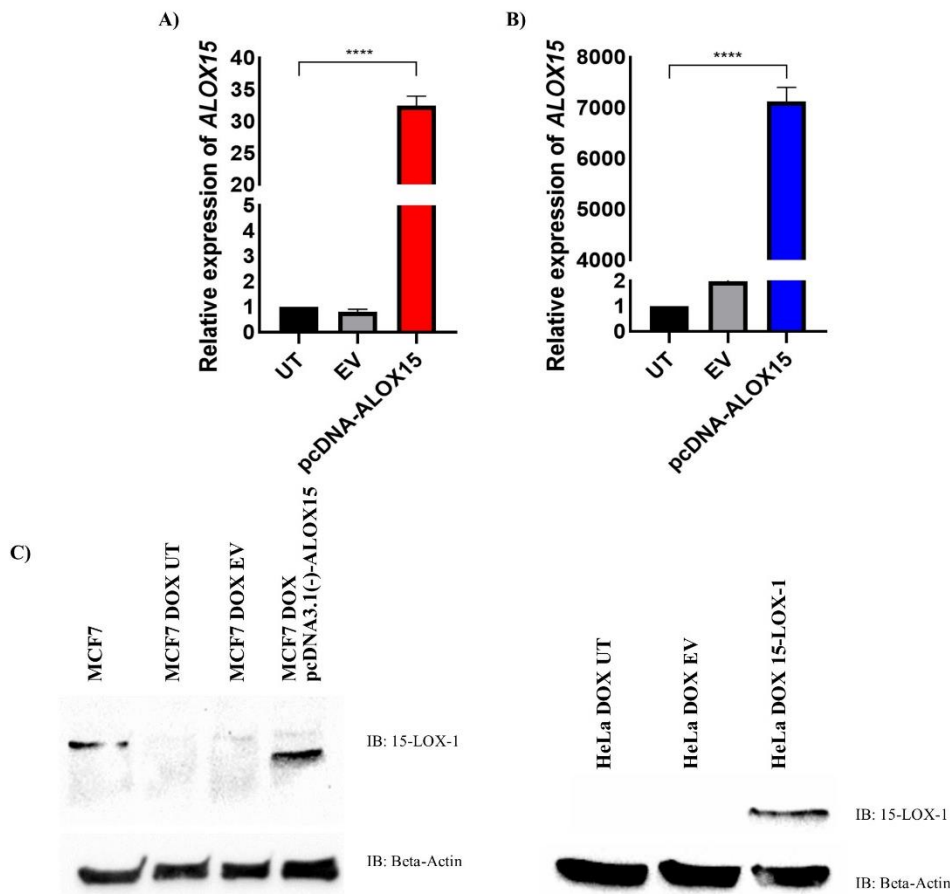
Figure 0-6 Over-expression of *ALOX15* in (A) MCF7 DOX and (B) HeLa DOX cells at mRNA level. C) Over-expression of 15-LOX-1 in MCF7 DOX and HeLa DOX cells at protein level.

3.6 Effect of 15-LOX-1 overexpression on cell viabilities

After the overexpression of 15-LOX-1 successfully performed, the effect of this manipulation on cells were followed by MTT assay or Western Blotting. For these assays, cells were seeded into 6- or 96-well plates, incubated for two days; cells were transfected with EV or pcDNA3.1(-)-ALOX15 in the presence of untreated control, incubated 48 h and assays were carried out. According to the results (Figure 3.8), the death with the 15-LOX-1 transfection was higher compared to untreated and UT

control in MCF7 DOX and HeLa DOX cells. Moreover, as 15-LOX-1 was one of the tumour suppressor proteins (Cimen et al., 2011), the overexpression of the 15-LOX-1 also induced apoptosis in sensitive MCF7 cells showed by the Western Blotting for Cleaved Caspase 3 protein which was a marker of the apoptosis (Smith et al., 2008). These results again emphasize the role of 15-LOX-1 as a tumour suppressor protein and its overexpression was enough to induce cell death mechanisms, specifically apoptosis in MCF7 cells.
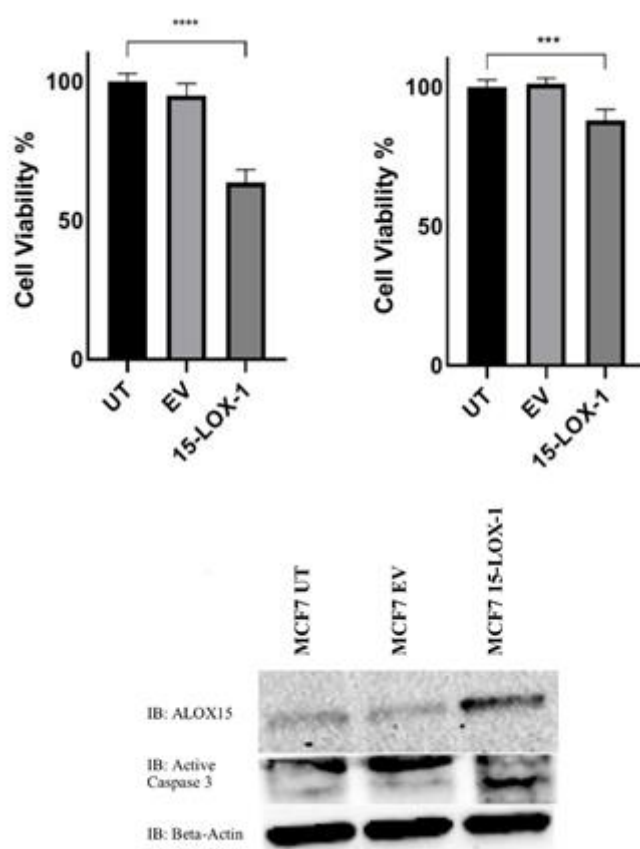
Figure 0-7 Effect of overexpression of 15-LOX-1 in cell viability and cell death. Upper left: MCF7 DOX cells were transfected with EV or pcDNA3.1(-)-ALOX15 and cell viabilities was followed by MTT assay. Upper right: HeLa DOX cells were transfected with EV or pcDNA3.1(-)-ALOX15 and cell viabilities was followed by MTT assay. Bottom: MCF7 cells were transfected with EV or pcDNA3.1(-)-ALOX15 and cleavage of Caspase 3 was figured out by Western Blotting.

3.7 Downregulation of 15-LOX-1 in sensitive cells

To further confirm the role of 15-LOX-1 in doxorubicin resistance, a shRNA vector, pSUPER-shALOX15 was designed by molecular cloning method according to the sequence information of the literature (Mumy et al., 2008). Next, colonies were scanned for insert-containing colonies by colony PCR (Figure 3.9). In addition to sh vector for 15-LOX-1 downregulation, a control vector, mock that did not contain any specific shRNA of any target protein was designed and used as control.
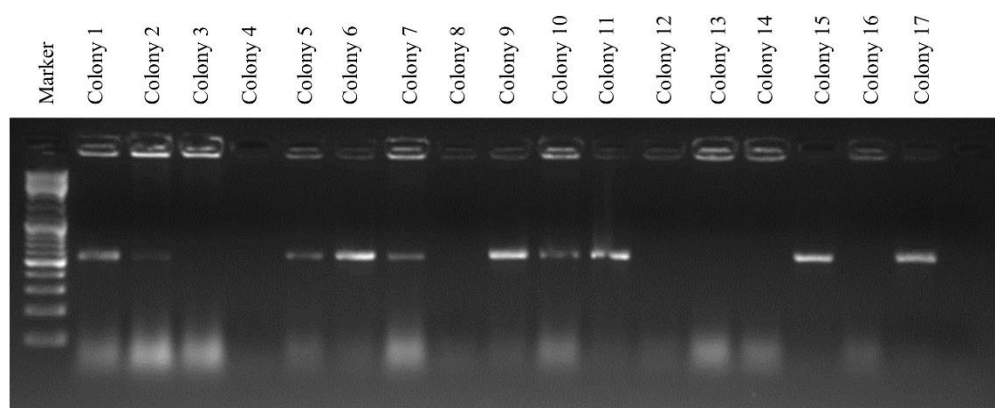
Figure 0-8 Result of colony PCR. The bands show the insert-positive colonies.

After the design of the shRNA vectors, MCF7 and HeLa sensitive cells were transfected with these vectors and expression of 15-LOX-1 was followed by qRT-PCR. The results showed that not only shRNA for 15-LOX-1 but also mock downregulated the 15-LOX-1, underlying that mock shRNA sequence also somehow targeted the *ALOX15* mRNA (Figure 3.10).
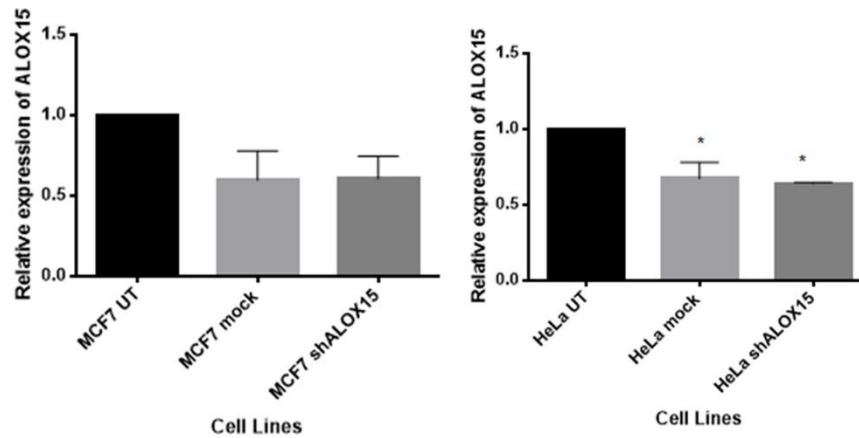
Figure 0-9 Downregulation of 15-LOX-1 by designed shRNA vectors.

To overcome this problem, the vector backbone, pSUPER was used as empty vector control instead of mock control. According to the results, 15-LOX-1 was successfully downregulated in MCF7 and HeLa cells compared to EV and untreated controls (Figure 3.11).
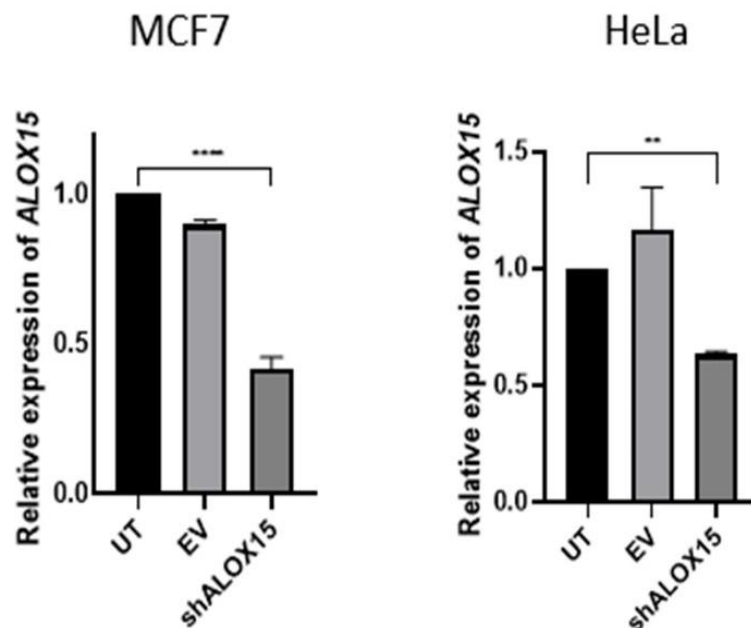
Figure 0-10 Downregulation of 15-LOX-1 by designed shRNA vector in the presence of untreated and EV controls.

After the downregulation of the 15-LOX-1 was shown, the effect of this downregulation on HeLa cells was assessed with the exceptation of that downregulation of 15-LOX-1 increases the cell viability and support resistance to doxorubicin in this cell line. However, suprisingly, the results figured out the reverse effect; the downregulation of the 15-LOX-1 increased the cell death and sensisitivty towards doxorubicin in sensitive HeLa cells (Figure 3.12). These result implied that transient silencing of the 15-LOX-1 was not informative in terms of cellular drug response and further long term effect should be followed to ensure the effect of the 15-LOX-1 silencing.
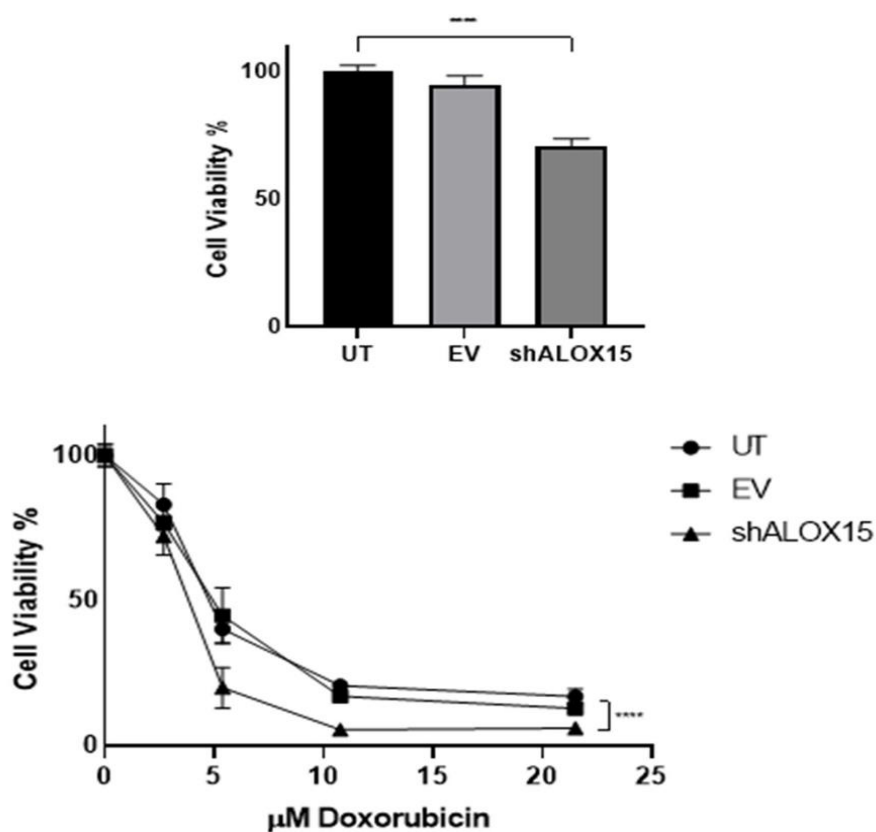
Figure 0-11 Effect of donwregulation of 15-LOX-1 in HeLa cells. HeLa cells were transfected with pSUPER-shALOX15 or EV and the cell viabilities were determined in the absence (top) and presence (bottom) of the doxorubicin.

3.8 Effect of 15-LOX-1 overexpression on response to doxorubicin

As the overexpression of 15-LOX-1 was proved by qRT-PCR and Western Blotting in MCF7 DOX and HeLa DOX cells, the effect of overexpression on response to doxorubicin was assessed by MTT cell viability assay. The overexpression of 15-LOX-1 partially re-sensitized these cells towards doxorubicin (Figure 3.13). This study is the first report defining a role for 15-LOX-1 in the doxorubicin resistance in cancer.
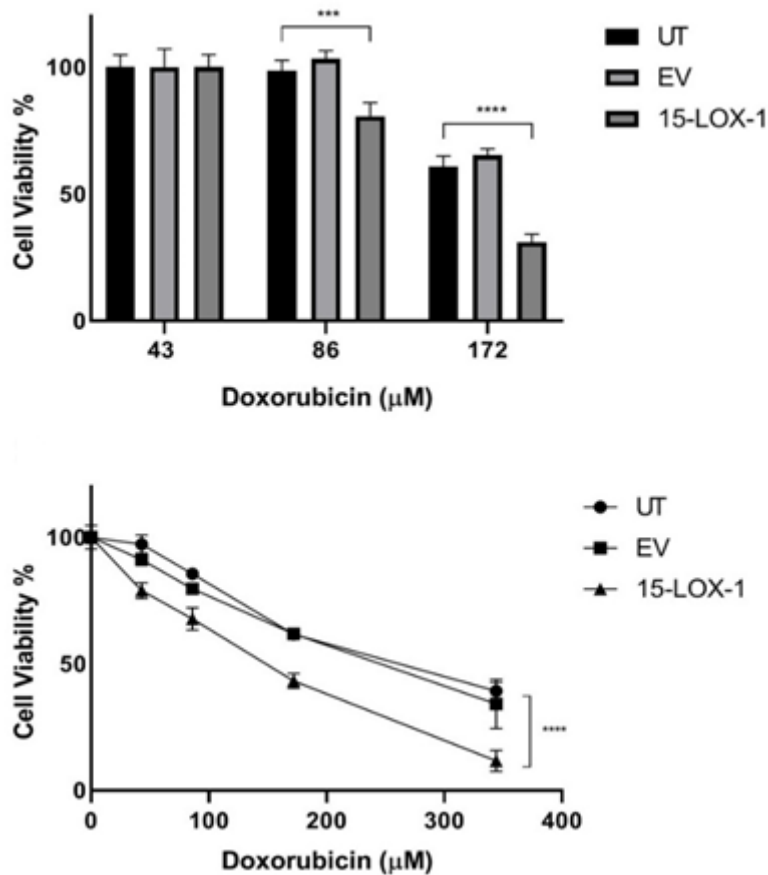
Figure 0-12 Effect of 15-LOX-1 overexpression on response to doxorubicin in MCF7 DOX (top) and HeLa DOX (bottom) cells. Doxorubicin-resistant MCF7 and HeLa cells were transfected with either empty (EV) or pcDNA3.1(-)-ALOX15 vector and treated with doxorubicin for 48 h after transfection. Cell viability was measured by MTT assay. Data were analysed with one-way ANOVA followed by post-hoc Tukey's test or non-linear regression analysis (***$p<0.001$; ****$p<0.0001$).

3.9 Effect of 15-LOX-1 overexpression on ABCB1 expression

Multidrug resistance protein, Pgp is the major factor that promotes doxorubicin resistance in MCF7 and HeLa DOX cells. Reversal of resistance phenotype may be directly linked Pgp function or expression. Donmez et al. showed that even the Pgp

blockers induced downregulation of *ABCB1* which was critical for the understanding of the function of the Pgp blockers (Donmez et al., 2011). Thus, any re-sensitization process could be a result of downregulation of the *ABCB1*.

The overexpression of 15-LOX-1 was illustrated to partially reverse the resistance in the doxorubicin-resistant MCF7 and HeLa cells. As the major mechanism of the resistance in MCF7 DOX and HeLa DOX cells is the overexpression of the *ABCB1* gene product, P-glycoprotein (P-gp; Figure 3.14) and the targeting and downregulation of the P-gp were shown to be a strategy to re-sensitize the cells towards different chemotherapeutics (Lima et al., 2007; Donmez and Gunduz, 2011; Abbasi et al., 2013), the possible effect of 15-LOX-1 overexpression on re-sensitization process could be downregulation of the P-gp.
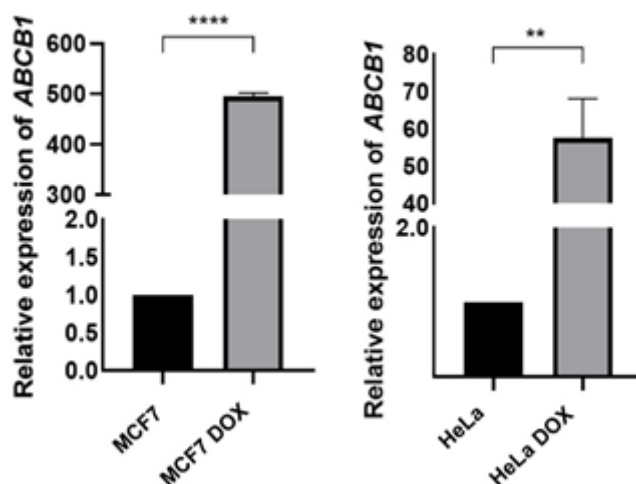
Figure 0-13 *ABCB1* expression in MCF7 DOX and HeLa DOX cells compared to their sensitive counterparts (**p<0.01; ****p<0.0001).

The overexpression of P-gp was shown to be major resistance mechanism as shown in Figure 3.14 in addition to copy number increase of the gene as discussed above. However, the overexpression of 15-LOX-1 did not alter the expression profile of the P-gp (Figure 3.15), pointing other mechanisms would be responsible for the partial re-sensitization process.
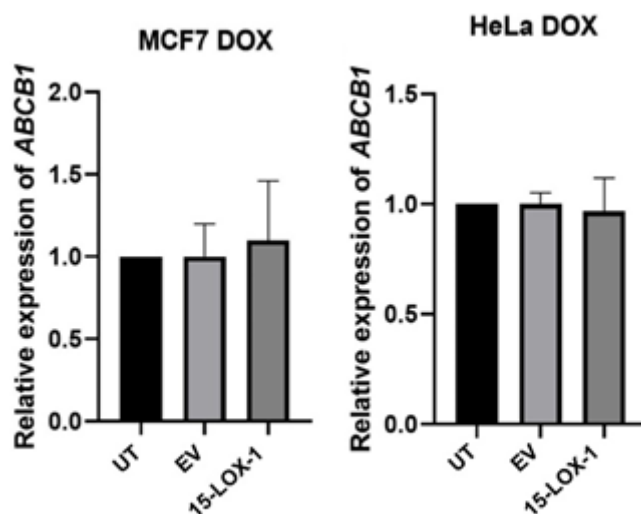
Figure 0-14 Effect of overexpression of 15-LOX-1 on expression of ABCB1. MCF7 DOX and HeLa DOX cells were transfected with pcDNA3.1(-)-ALOX15 or EV in the presence of untreated control. ABCB1 expression was determined by qRT-PCR.

3.10 Effect of 15-LOX-1 overexpression on intracellular doxorubicin accumulation in doxorubicin-resistant cells

Even though the expression of P-gp was not regulated by 15-LOX-1, its activity can be affected by 15-LOX-1. Membrane fluidity and lipids can limit the function of P-gp (Dos Santos et al., 2007; Sharom, 2014). Thus, the activity of P-gp was aimed to be studied. Doxorubicin is a fluorescent dye with an emission in the red region (Karukstis et al., 1998). Thus, its localization could be followed fluorescently. Intracellular accumulation of doxorubicin could be a measure of the function of the P-gp. Hence, intracellular doxorubicin accumulation was determined in MCF7 DOX and HeLa DOX cells overexpressing 15-LOX-1 in the presence of EV control. The results showed that the accumulation of doxorubicin was increased in 15-LOX-1-overexpressing MCF7 DOX cells compared to EV control but not in HeLa DOX cells (Figure 3.16). 15-LOX-1 can oxygenate the membrane polyunsaturated fatty

acids in the free or membrane-bound form (Walther et al., 2002). Therefore, it can reorganize the cell membrane lipids and fluidity. In the hypothesis, 15-LOX-1 increases the cell membrane fluidity by modifying the membrane lipids and increased membrane fluidity limits the function of the P-gp exporter (Sinicrope et al., 1992; Sharom, 1997; Hendrich and Michalak, 2003). This case was valid just for MCF7 DOX cells; however, HeLa DOX cells did not affected in terms of P-gp function and other mechanisms that will be discuss in the other sections could be responsible for the partial re-sensitization of the HeLa DOX cells when they overexpressed 15-LOX-1.
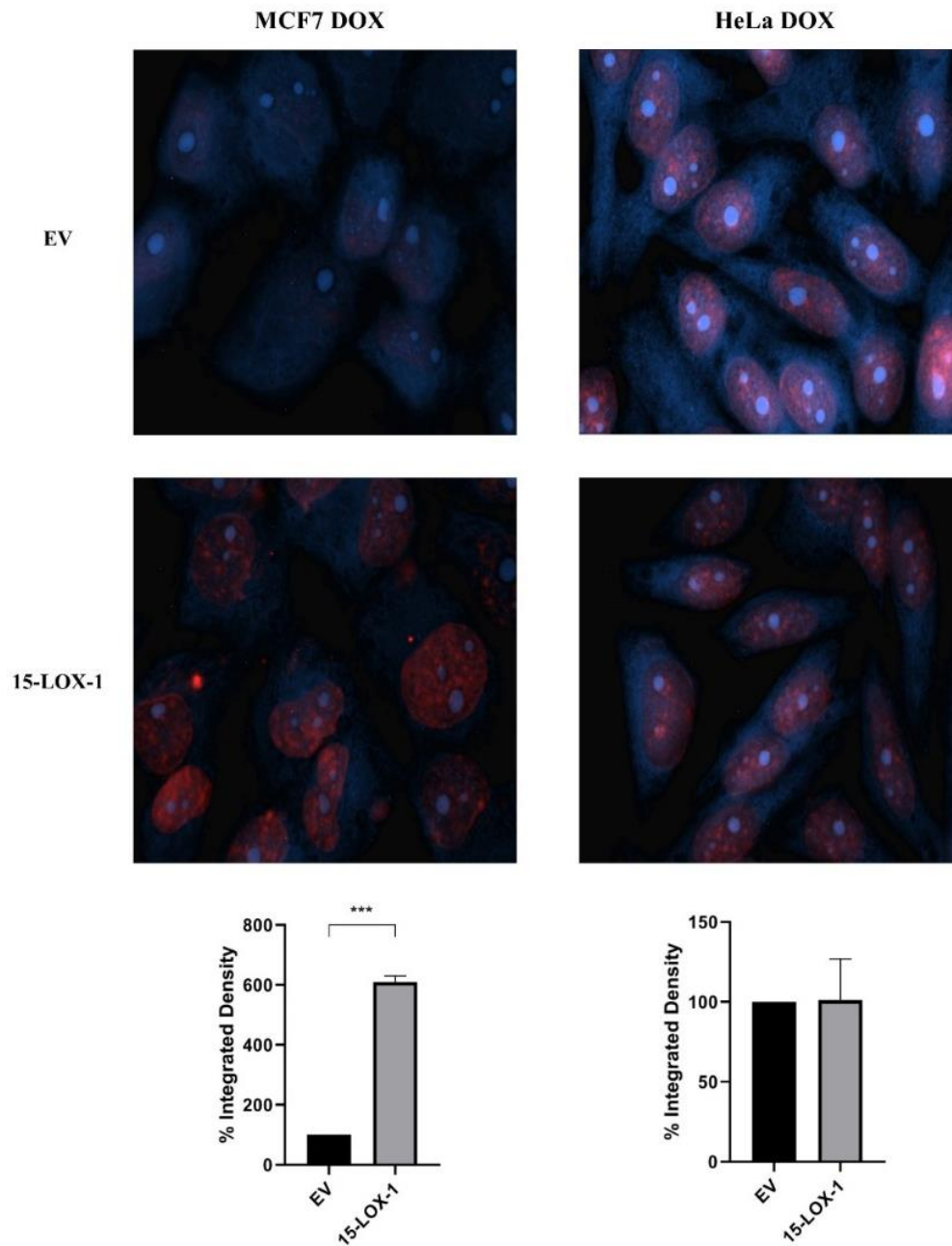
Figure 0-15 Intracellular doxorubicin accumulation in MCF7 DOX and HeLa DOX cells overexpressing 15-LOX-1. Doxorubicin-resistant MCF7 and HeLa cells were transfected with either empty (EV) or pcDNA3.1(-)-ALOX15 expression vector for 48 h, treated with 10 μM doxorubicin and stained with CellTrackerTM Blue CMAC. The integrated density plots were obtained via red-only fluorescence. Data were analysed with one-way ANOVA followed by post-hoc Tukey's test (***$p<0.001$).

3.11 Effect of 15-LOX-1 overexpression on motilities of the doxorubicin-resistant cells

To test the hypothesis of that 15-LOX-1 increased the membrane fluidity in MCF7 DOX cells but not in HeLa DOX cells, the motilities of these cells were determined when they expressed the 15-LOX-1 or not. Membrane dynamics have previously been correlated to the tumour aggressiveness including cellular motility (Taraboletti et al., 1989; Sade et al., 2012). Hence, the motility was implicated to give an idea about the fluidity of the cell membrane. Cellular motility was examined for four days by *in vitro* wound healing assay (Rodriguez et al., 2005). The results underlined that the motility of MCF7 DOX cells increased when they overexpressed 15-LOX-1. This effect was not seen in HeLa DOX cells even they overexpressed 15-LOX-1 (Figure 3.17). Overall, it can be stated that 15-LOX-1 increased the cell motility and membrane fluidity and limited the function of P-gp in MCF7 DOX cells but not in HeLa DOX cells.
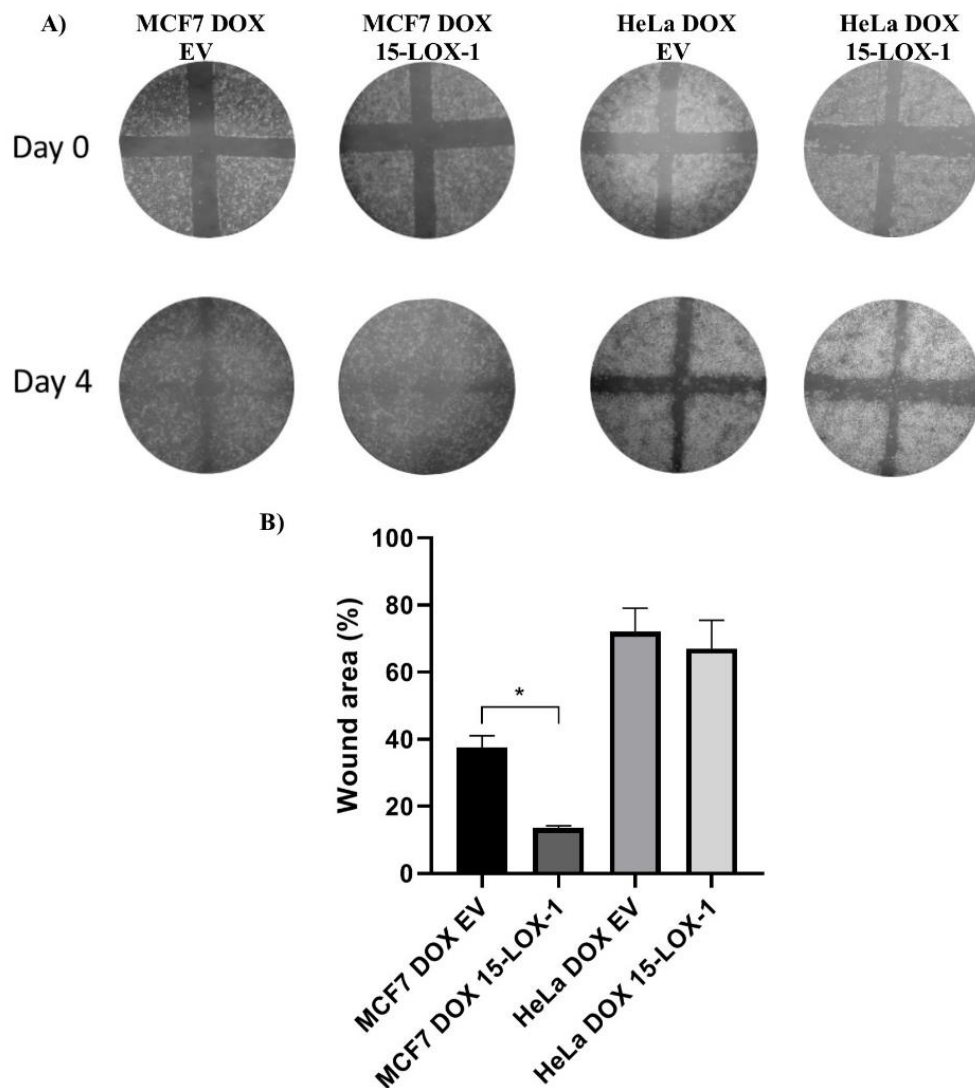
Figure 0-16 Effect of 15-LOX-1 overexpression on cell motility. A) Representative figure for *in vitro* wound healing assay in MCF7 DOX and HeLa DOX cells transfected with pcDNA3.1(-)-ALOX15 or EV. B) The graph of the length of the wounds compared to day 0 where the lengths were assumed as 100%. Data were analysed with t-test. *$p<0.05$.

The motility of cells could be linked to metastasis and thus cancer aggressiveness (Birchmeier et al., 2003; Palmer et al., 2011). However, motility is a property of the epithelial cells during the epithelial-to-mesenchymal transition from which carcinogenesis takes place (Jogi et al., 2012). Thus, 15-LOX-1 over-expression may

trigger the dedifferentiation of the MCF7 DOX cells to epithelial, a less aggressive form of the carcinogenesis.

3.12 Effect of 15-LOX-1 overexpression on cell cycle distributions of doxorubicin-resistant cells

The major product of the 15-LOX-1-mediated reaction, 13(S)-HODE was previously shown to trigger cell cycle arrest (Tavakoli-Yaraki and Karami-Tehrani, 2013). Thus, to further explore the role of 15-LOX-1 in doxorubicin resistance, the cell cycle status were followed by Flow cytometer (Figure 3.18).
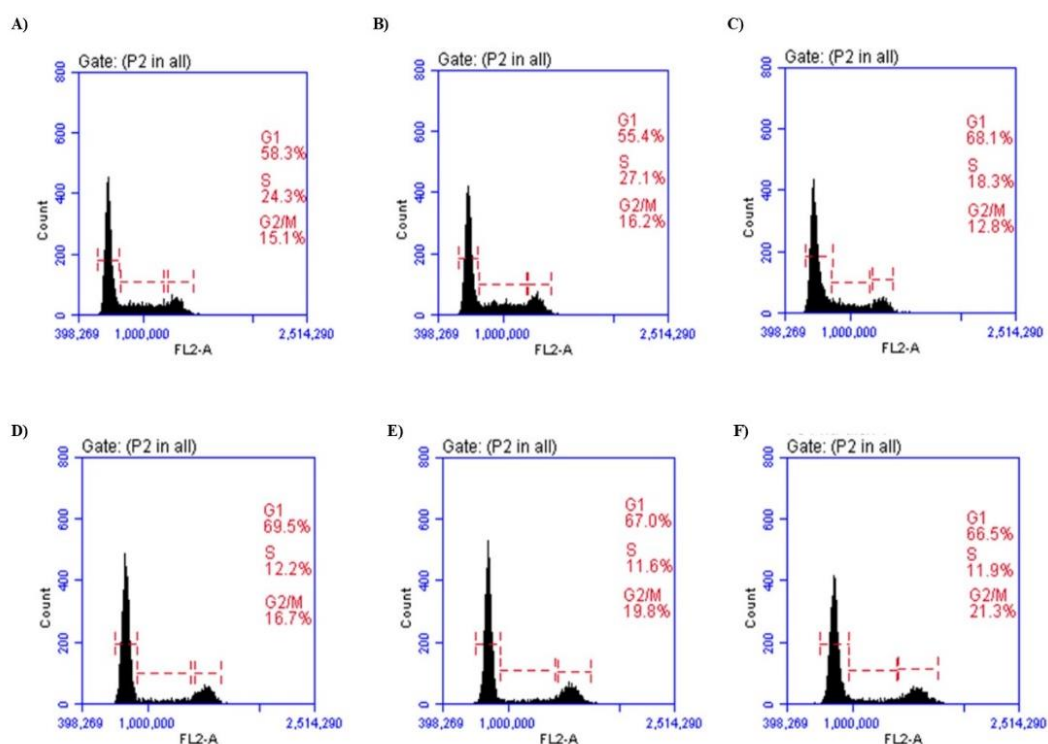
Figure 0-17 Representative figure for cell cycle analysis of (A) un-transfected (UT), (B) empty vector (EV)-transfected and (C) pcDNA3.1(-)-ALOX15-transfected MCF7 DOX cells and (D) un-transfected (UT), (E) empty vector (EV)-transfected and (F) pcDNA3.1(-)-ALOX15 transfected HeLa DOX cells.

Cell cycle analyses revealed that 15-LOX-1 overexpressing MCF7 DOX cells accumulated in the G1 phase while the accumulation of the cells in S and G2 phases slightly decreased (Figure 3.19). The accumulation in G1 phase implied that 15-LOX-1 overexpression caused G1 arrest in MCF7 DOX cells. However, the overexpression of 15-LOX-1 did not affect the cell cycle status of the HeLa DOX cells contrary to MCF7 DOX cells. These results underlined the importance of the 15-LOX-1 expression cell cycle regulation in MCF7 DOX cells but not in HeLa DOX cells.
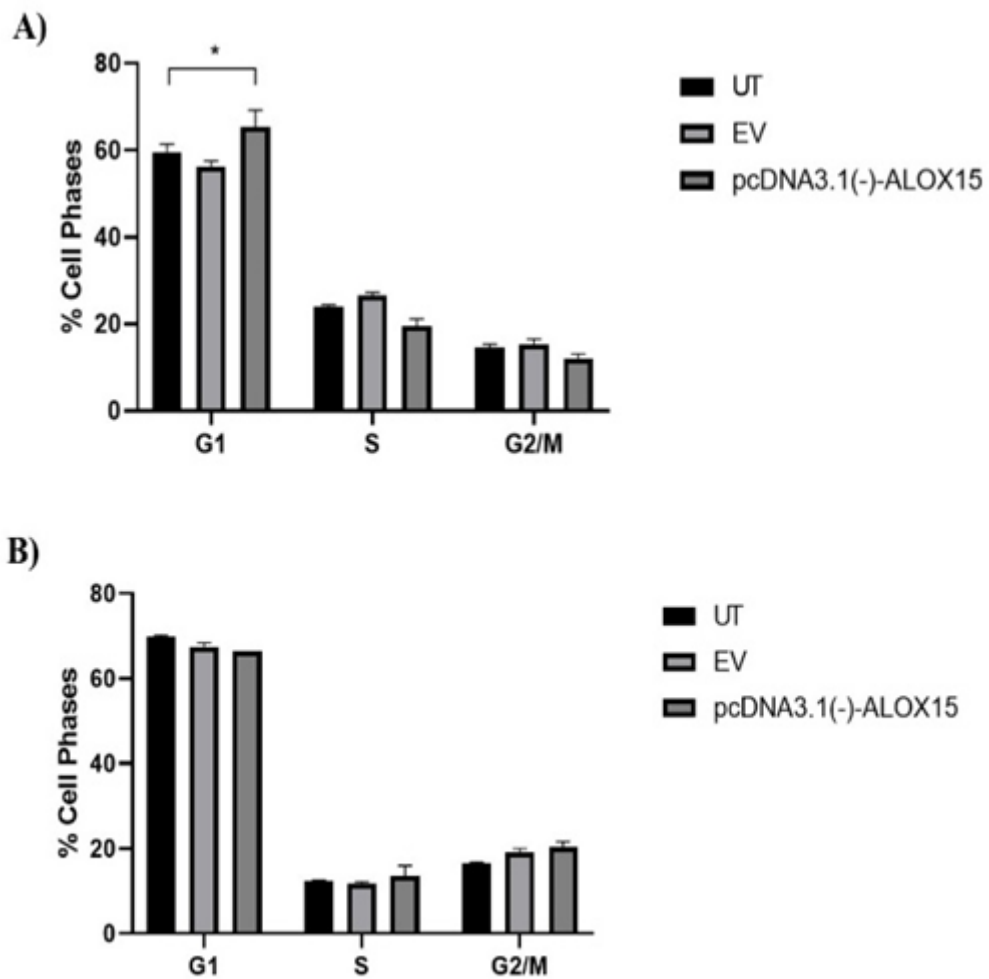
Figure 0-18 Cell cycle status of 15-LOX-1-overexpressing MCF7 DOX (A) and HeLa DOX (B) cells. Cycle of the cells were determined by Flow cytometer and quantified and graphed according to the Figure 3.18. *p<0.05.

3.13 Effect of 15-LOX-1 overexpression on apoptosis in the doxorubicin-resistant cells

Apoptosis is a fundamental cell death mechanism and resistance to apoptosis is one of the strategies of the cells to resist the chemotherapeutics. Thus, targeting apoptosis-related pathways could be an alternative to overcome the cancer drug

resistance (Tsuruo et al., 2003). To check the effect of 15-LOX-1 overexpression on apoptosis in MCF7 DOX and HeLa DOX cells, a Caspase 3/7 assay was used. Executioner Caspases 3 and 7 are the critical markers of the apoptosis (Smith et al., 2008); hence, any alterations in the activity of these caspases could be linked to apoptosis. The increase in the fluorescent signal in the caspase assay indicates higher Caspase 3/7 activity, thus enhanced apoptosis. The results showed that the Caspase 3/7 activity was significantly increased in MCF7 DOX cells when they overexpressed 15-LOX-1. The results indicated that 15-LOX-1 expression alone was sufficient to trigger apoptosis in MCF7 DOX cells. Treatment with Etoposide (ETO), a well-known apoptosis inducer, enhanced this effect, further stimulating apoptosis in 15-LOX-1 overexpressing MCF7 DOX cells (Figure 3.20). The overexpression of 15-LOX-1 alone in HeLa DOX cells did not trigger apoptosis. However, ETO treatment induced the apoptosis in 15-LOX-1 expressing HeLa DOX cells compared to ETO-treated EV control group in HeLa DOX cells (Figure 3.20). This indicated that in HeLa DOX cells, 15-LOX-1 expression can induce apoptosis only in the presence of an apoptotic signal.
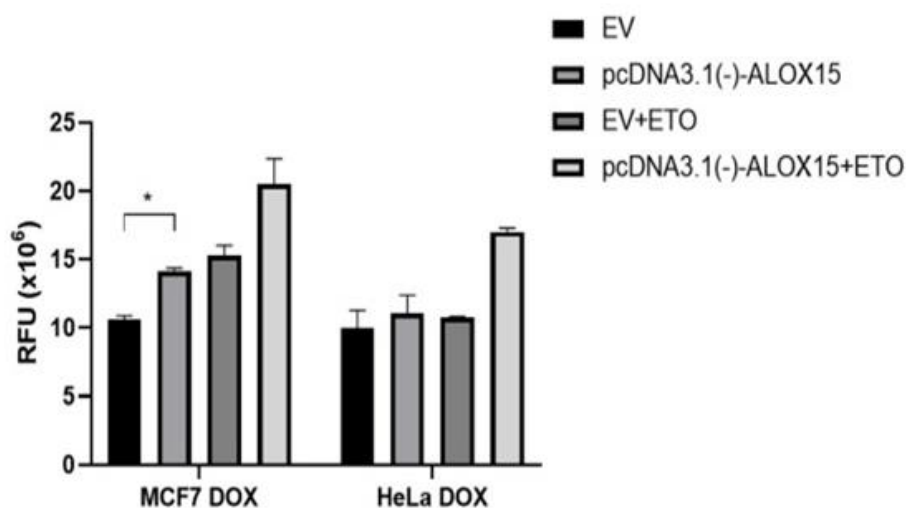
Figure 0-19 Effect of 15-LOX-1 overexpression on apoptosis in MCF7 DOX and

HeLa DOX cells. Apoptosis was followed by Caspase 3/7 assay. Etoposide (ETO) was used as an inducer of the apoptosis. *p<0.05.

15-LOX-1 has previously been linked to apoptosis due to the final member of the apoptosis-related pathway, PPARγ that blocks nuclear factor-kappa B (NF- κB) and activates several apoptosis-related genes (Cimen et al., 2011; Tavakoli-Yaraki and Karami-Tehrani, 2013). Therefore, the present findings were parallel to the literature and questioned the expression and activity of the PPARγ protein.

3.14 Effect of PPARγ on apoptosis in sensitive and doxorubicin-resistant cells

The main product of the 15-LOX-1-mediated reaction, 13(S)-HODE is a substrate for the orphan receptor, PPARγ. PPARγ can activate apoptosis (Cimen et al., 2011) and the previous findings could be linked to PPARγ function. Thus, the expression of the *PPARG* was firstly determined by qRT-PCR in MCF7 DOX and HeLa DOX cells compared to their drug-sensitive counterparts. According to the results, the *PPARG* was significantly downregulated in MCF7 DOX cells compared to parental MCF7 cell line (Figure 3.21). However, the expression of *PPARG* was not detectable in both parental and doxorubicin-resistant HeLa cells, which explains why apoptosis could not be triggered by 15-LOX-1 overexpression in HeLa DOX cells.
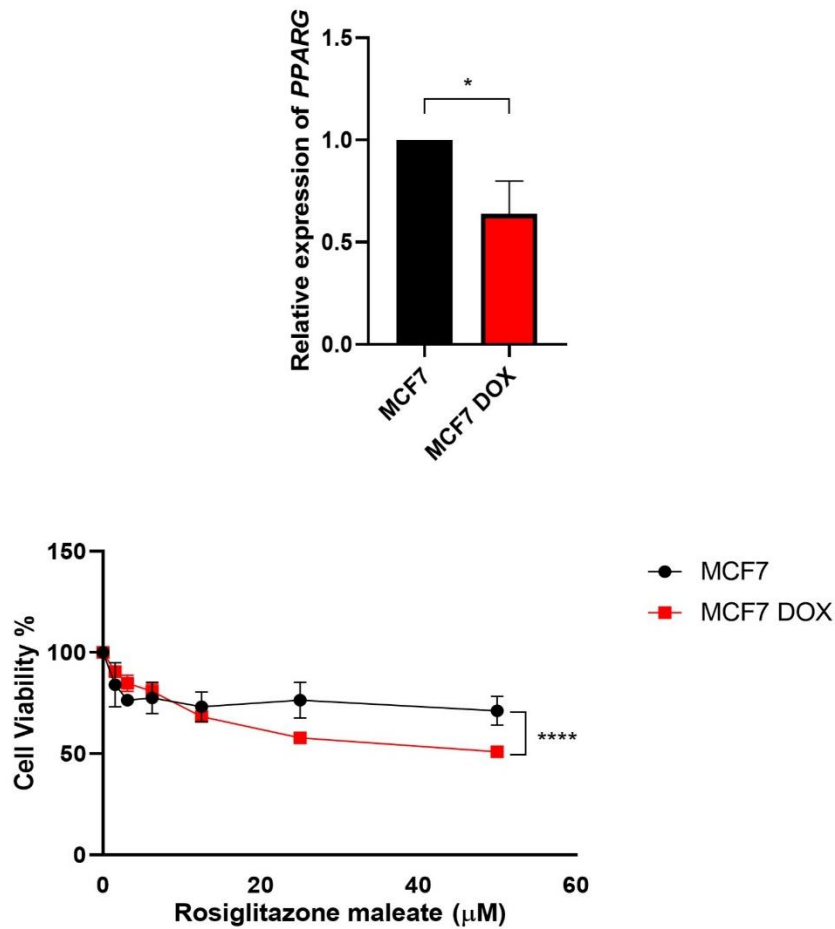
Figure 0-20 *PPARG* expression and effect of Rosiglitazone on cell death in MCF7 and MCF7 DOX cells.

To assess the function of PPARγ in detail, MCF7 and MCF7 DOX cells were treated with a PPARγ agonist, Rosiglitazone (GlaxoSmithKline, USA; Cuzzocrea et al., 2004). The results demonstrated that the Rosiglitazone was more effective in MCF7 DOX cells by activating the limited amount of the PPARγ protein (Figure 3.21). These results emphasized that targeting PPARγ directly by Rosiglitazone and indirectly by 15-LOX-1 overexpression could induce cell death in MCF7 DOX cells.

To further study the involvement of PPARγ in to 15-LOX-1-mediated cell death in the cell lines, a non-steroidal anti-inflammatory drug (NSAID), Dexday

(Dexketoprofen) was used. NSAIDs are known to increase the activity of 15-LOX-1 (Shureiqi et al., 2000). Hence, an indirect effect of Dexday could reflect the possible role of 15-LOX-1. Therefore, MCF7 and MCF7 DOX cells were treated with different concentrations of Dexday and the alterations in cell viability were monitored by MTT assay.
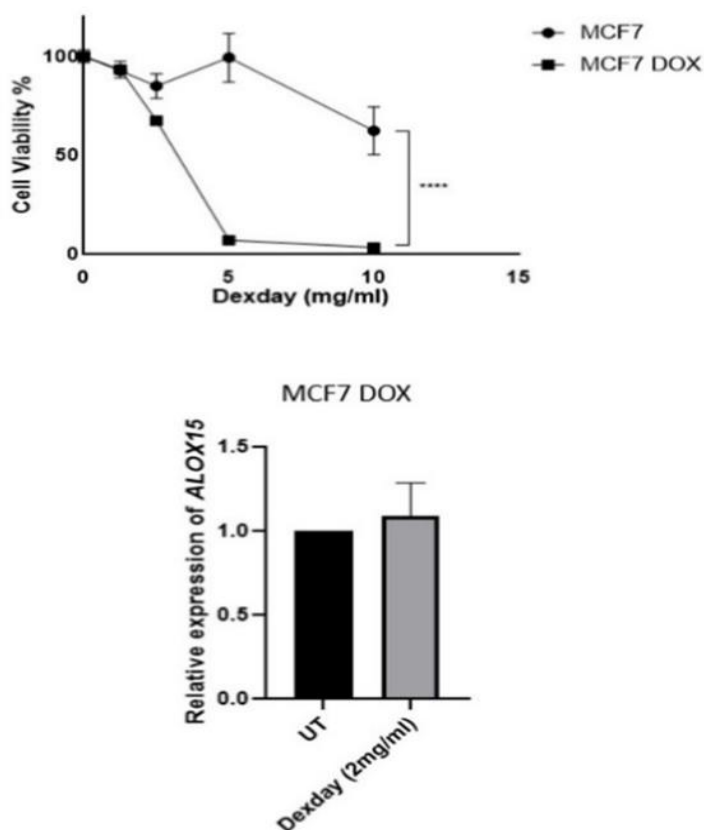
Figure 0-21 Effect of Dexday on cell viabilities of sensitive and doxorubicin-resistant cell lines and on 15-LOX-1 expression in MCF7 DOX cells. ****$p<0.0001$.

The results demonstrated that similar to the effect of Rosiglitazone, Dexday treatment also significantly induced cell death in MCF7 DOX cells compared to parental MCF7 cells (Figure 3.22). The effect was not a result of increased expression of 15-LOX-1 but could be a result of increased activity of 15-LOX-1. The activity and expression of 15-LOX-1 were reported to be not correlated (Camp et al., 1999). Therefore, these results emphasize the critical role of 15-LOX-1 in apoptosis

putatively via PPARγ function. Still, detailed molecular studies on Dexday and/or other NSIDs are needed to completely explore the roles of these drugs on cancer drug resistance in combination of 15-LOX-1 and PPARγ functions.

3.15 Effect of 13(S)-HODE treatment on viabilities of the doxorubicin-resistant cells

As a major product of 15-LOX-1-mediated reaction, 13(S)-HODE plays critical roles in induction of apoptosis (Cimen et al., 2011). To further explore the effect of 13(S)-HODE on MCF7 DOX and HeLa DOX cells, these cells were treated with a low concentration of 13(S)-HODE in the presence of solvent control. According to the results, low concentration 13(S)-HODE treatment increased cell death in MCF7 DOX cells but not in HeLa DOX cells (Figure 3.23). These findings correlated with the previous ones as 13(S)-HODE showed its effect on cell viability putatively via PPARγ which was expressed in MCF7 DOX cells but not in HeLa DOX cells.
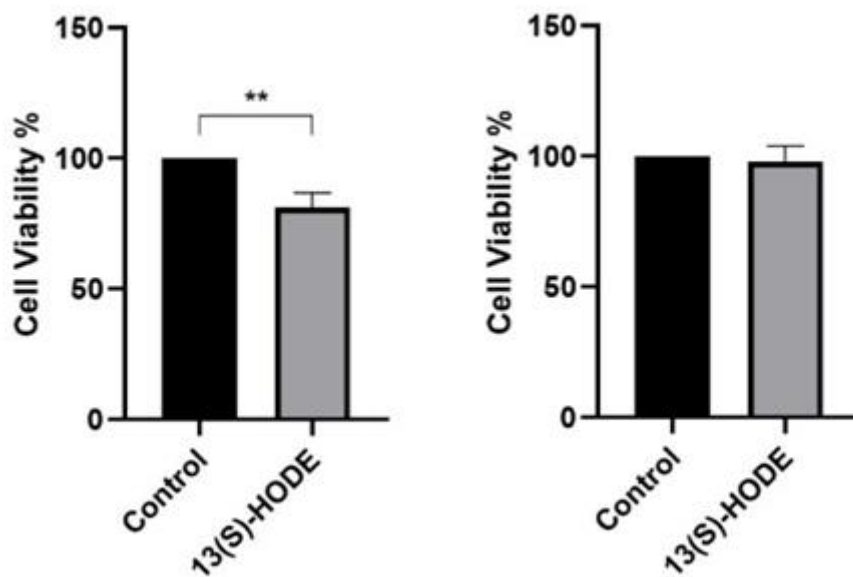
Figure 0-22 Effect of low concentration 13(S)-HODE treatments on MCF7 DOX and HeLa DOX cells. The cells were treated by 0.5 µg/ml of 13(S)-HODE and cell viabilities were followed by MTT assay. Left: MCF7 DOX; Right: HeLa DOX cells. Data were analysed by t-test. **p<0.01.

3.16   Effect of 13(S)-HODE treatment on response to doxorubicin

The effect of 13(S)-HODE was further analysed by concerning the resistance status. For this aim, the cells were treated with both 13(S)-HODE and increasing concentrations of doxorubicin. 13(S)-HODE treatment partially re-sensitized the doxorubicin resistance in HeLa DOX cells but not in MCF7 DOX cells (Figure 3.24).
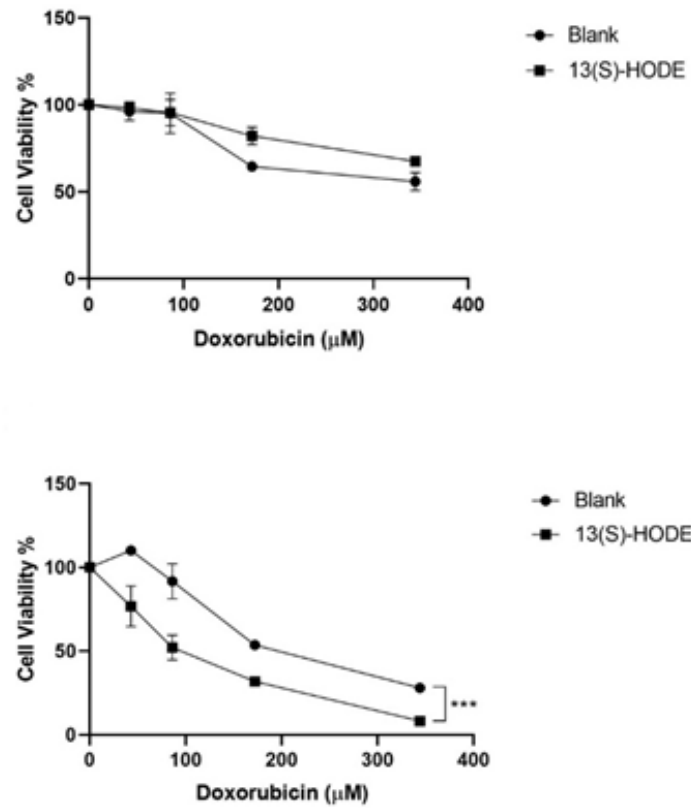
Figure 0-23 Effect of 13(S)-HODE treatment on response to doxorubicin in MCF7 DOX (top) and HeLa DOX (bottom). Cells were treated with doxorubicin at increasing concentrations and 13(S)-HODE, and cell viabilities were determined by MTT assay. Data were analysed by non-linear regression. ***$p < 0.001$.

This result emphasized that 15-LOX-1 re-sensitized the HeLa DOX cells but its major reaction product, 13(S)-HODE. This effect could be a result of the stimulation of another cell death mechanism, ferroptosis, which is guided by reactive oxygen and lipid species. 15-LOX-1 was previously proved to be involved in ferroptotic cell death pathway (Yang et al., 2016; Gaschler and Stockwell, 2017). Still, further molecular studies are needed to conclude such a hypothesis.

3.17   15-LOX-1 and PPARγ expressions in human cancer samples

The effects of 15-LOX-1 and PPARγ on response to the drugs were also questioned in different human cancer samples. The data obtained from TCGA (https://www.cancer.gov/tcga) showed the analyses of samples from non-treated cancer patients (https://www.cancer.gov/tcga). The patients then were administered different anti-cancer drugs with defined time periods and dosages, and the progression was summarized as clinical progressive disease, stable disease, partial response and complete response.

The data were analysed by separating the patient sample results into three groups: clinical progressive disease, stable disease and partial or complete response for breast cancer patients and doxorubicin administration. The expression values of *ALOX15* and *PPARG* were obtained by cBioPortal (Cerami et al., 2012; Gao et al., 2013) and graphed according to the given groups. The results showed that there was an increase in the expressions of *ALOX15* and *PPARG* when the drugs were effective and the response was partial or complete compared to stable and progressive disease (Figure 3.25). These results underlined the importance of 15-LOX-1 and PPARγ on response to the drugs.
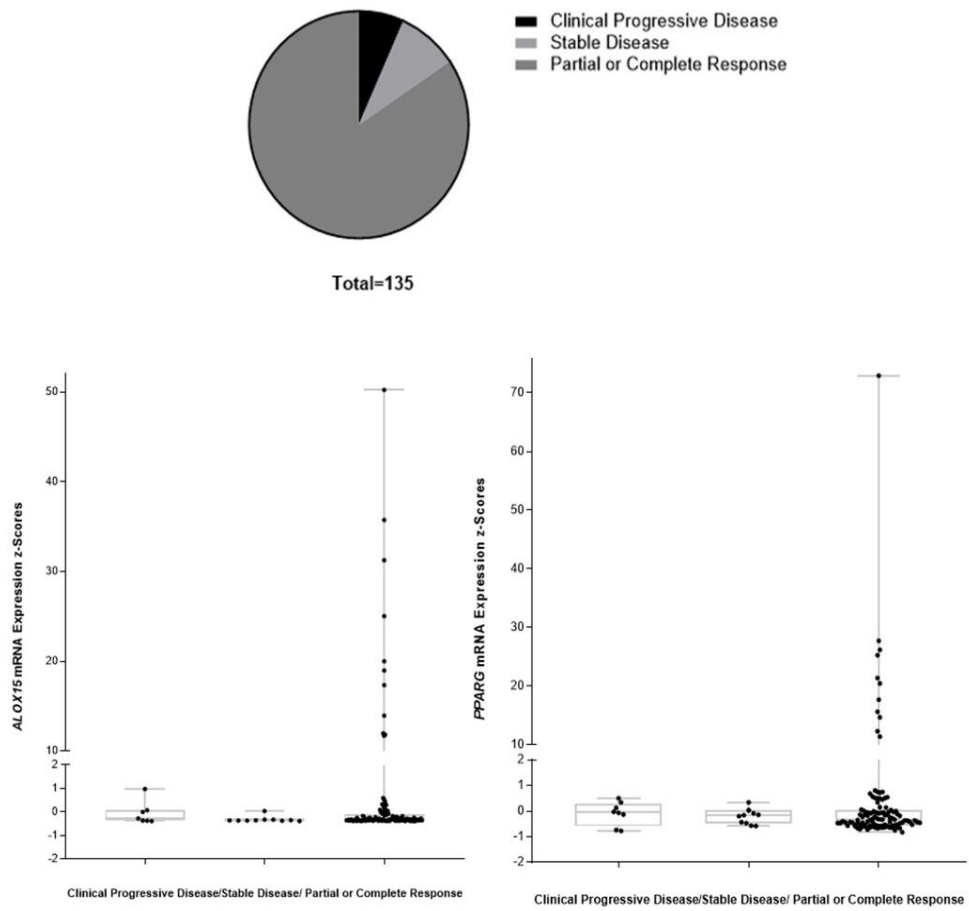
Figure 0-24 Analyses of TCGA data. 135 patient samples that were diagnosed by breast cancer and administered doxorubicin after obtaining the RNA-Seq data were analysed as three groups: clinical progressive disease, stable disease and partial or complete response. The data were obtained from CBioPortal using patient TCGA ID. The data were analysed by One-Way Anova and was significant when $p<0.05$.

CHAPTER 4

CONCLUSIONS

Drug resistance in cancer is a phenomenon that limits the efficacy of the treatment of cancer. There have been several reasons reported to promote cancer drug resistance. Although well-defined mechanisms are targeted to overcome drug resistance, novel mechanisms should be investigated to prevent cancer drug resistance and relapse of the cancer. Enzymatic pathways are critically important to target as they can be blocked or activated small molecule treatment. Thus, it is easy to adapt the academic findings to the clinics. The enzymes that have not yet been associated to cancer drug resistance is fundamental as novel co-therapy approaches could be developed.

15-LOX-1 is an important enzyme oxygenating membrane polyunsaturated fatty acids. Due to this function, it is involved in the regulation of different physiological conditions. However, disruption of 15-LOX-1-mediated reaction could result in pathophysiological conditions one of which is the cancer.

In the present study, the role 15-LOX-1 in cancer drug resistance was examined in detail for the first time. The results underlined that 15-LOX-1 was downregulated in doxorubicin-resistant MCF7 and HeLa cells; however, this was cell and/or drug specific. Moreover, overexpression of 15-LOX-1 decreased the cell viability in these cell lines and partially re-sensitized the resistant cells to doxorubicin. The effect was seen to be cell-specific. 15-LOX-1 caused membrane reorganization by putatively altering the membrane fluidity, G1 arrest and apoptosis in MCF7 DOX cells. Nonetheless, these phenotypic changes could not be observed in HeLa DOX cells. Also, the apoptosis was shown to be a result of PPARγ activation in MCF7 DOX cells while it was completely silenced in HeLa DOX cells. Surprisingly, contrary to MCF7 DOX cells, the major product of 15-LOX-1-mediated reaction, 13(S)-HODE

was effective in terms of re-sensitization in HeLa DOX cells. This could be a result of putatively increased reactive lipid species in HeLa DOX cells. Thus, 15-LOX-1 seemed to have two different effects on these cell lines (Figure 4.1). 15-LOX-1 reorganized the membrane fluidity and triggered apoptosis in MCF7 DOX cells but putatively increased the reactive lipid and oxygen species in HeLa DOX cells.
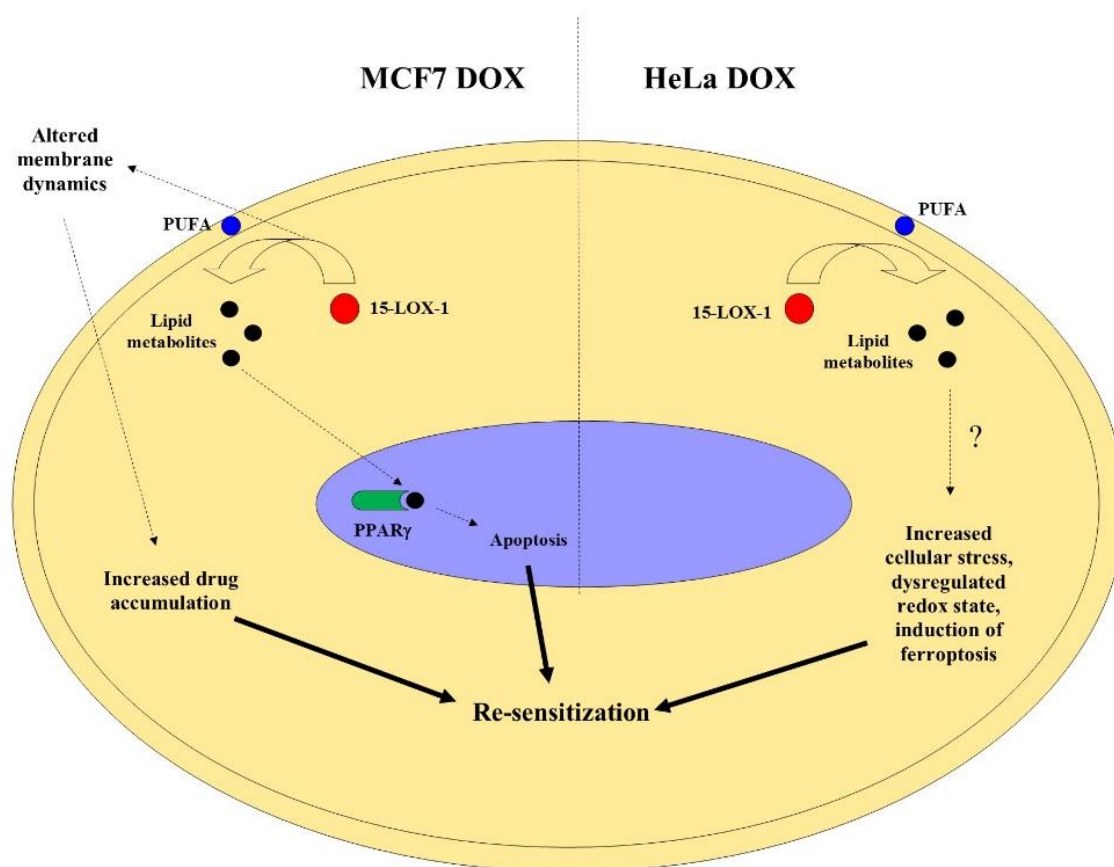
Figure 0-1 Proposed mechanisms for 15-LOX-1 in MCF7 DOX and HeLa DOX cells to re-sensitize the doxorubicin resistance.

CHAPTER 5

FUTURE PERSPECTIVES

The present study proposed possible mechanisms of 15-LOX-1 in re-sensitization of doxorubicin resistance in MCF7 DOX and HeLa DOX cells.

The downregulation of 15-LOX-1 was expected to increase cell viability and resistance to doxorubicin in drug-sensitive parental cell lines. However, transient transfection of shRNA, which was specific to *ALOX15* by the mammalian vector, did not meet the expectations and a reverse effect was displayed. This experimental approach is required to be further tested by stable transfection to completely decipher the effect of *ALOX15* downregulation on cell phenotypes.

Although the mechanism of 15-LOX-1 was clearly explained for MCF7 DOX cells, that for HeLa DOX cells is controversial and require further studies. The preliminary data for ferroptotic cell death studies, which could be proposed for HeLa DOX cells while effects of 15-LOX-1 was considered, figured out that the ferroptosis was not affected by the 15-LOX-1. Still, further approaches and tests are needed to completely explore the role of 15-LOX-1 in ferroptosis in HeLa DOX cells.

REFERENCES

Abbasi, M., Lavasanifar, A., Uludag, H. (2013). Recent attempts at RNAi-mediated P-Glycoprotein downregulation for reversal of multidrug resistance in cancer. Medicinal Research Reviews, 33(1), 33-53.

American Cancer Society. (2017). Cancer Facts & Figures 2017. Atlanta: American Cancer Society; 2017.

Bailey, J. M., Makheja, A. N., Lee, R., & Simon, T. H. (1995). Systemic activation of 15-lipoxygenase in heart, lung, and vascular tissues by hypercholesterolemia: relationship to lipoprotein oxidation and atherogenesis. Atherosclerosis, 113(2), 247-258.

Baran, Y., Bielawski, J., Gunduz, U., & Ogretmen, B. (2011). Targeting glucosylceramide synthase sensitizes imatinib-resistant chronic myeloid leukemia cells via endogenous ceramide accumulation. Journal of cancer research and clinical oncology, 137(10), 1535.

Barrera, G. (2012). Oxidative stress and lipid peroxidation products in cancer progression and therapy. ISRN oncology, 2012.

Barrera, G., Pizzimenti, S., & Dianzani, M. U. (2008). Lipid peroxidation: control of cell proliferation, cell differentiation and cell death. Molecular aspects of medicine, 29(1-2), 1-8.

Berghe, T.V., Linkermann, A., Jouan-Lanhouet, S., Walczak, H., Vandenabeele, P. (2014). Regulated necrosis: the expanding network of non-apoptotic cell death pathways. Nature Reviews Molecular Cell Biology, 15, 135–147.

Bertram, J. S. (2000). The molecular biology of cancer. Molecular Aspects of Medicine, 21(6), 167-223.

Bhattacharya, S., Mathew, G., Jayne, D. G., Pelengaris, S., & Khan, M. (2009). 15-Lipoxygenase-1 in colorectal cancer: a review. Tumor Biology, 30(4), 185-199.

Birchmeier, C., Birchmeier, W., Gherardi, E., & Woude, G. F. V. (2003). Met, metastasis, motility and more. Nature reviews Molecular cell biology, 4(12), 915-925.

Bosch, I., & Croop, J. (1996). P-glycoprotein multidrug resistance and cancer. Biochimica et Biophysica Acta (BBA)-Reviews on Cancer, 1288(2), F37-F54.

Brash, A.R. (1999). Lipoxygenases: Occurrence, functions, catalysis, and acquisition of substrate. The Journal of Biological Chemistry, 274, 23679-82.

Camp, H.S., Whitton A.L., Tafuri, S.R. (1999). PPAR☐ activators down-regulate the expression of PPARG in 3T3-L1 adipocytes. FEBS Letters, 186, 186-190.

Cerami, E., Gao, J., Dogrusoz, U., Gross, B. E., Sumer, S. O., Aksoy, B. A., ... & Antipin, Y. (2012). The cBio cancer genomics portal: an open platform for exploring multidimensional cancer genomics data. Cancer Discov 2: 401–404.

Chen, Y., Peng, C., Abraham, S.A., Shan, Y., Guo, Z., Desouza, N., Cheloni, G., Li, D., Holyoake, T.L., Li, S. (2014). Arachidonate 15-lipoxygenase is required for chronic myeloid leukemia stem cell survival. The Journal of Clinical Investigations, 124(9), 3847-62.

Choi, J., Chon, J. K., Kim, S., & Shin, W. (2008). Conformational flexibility in mammalian 15S-lipoxygenase: Reinterpretation of the crystallographic data. Proteins: Structure, Function, and Bioinformatics, 70(3), 1023-1032.

82

Cimen, I., Tuncay, S., Banerjee, S. (2009). 15-Lipoxygenase-1 expression suppresses the invasive properties of colorectal carcinoma cell lines HCT-116 and HT-29. Cancer Science, 100(12), 2283-91.

Cimen, I., Astarci, E., Banerjee, S. (2011). 15-Lipoxygenase-1 exerts its tumor suppressive role by inhibiting nuclear factor-kappa B via activation of PPAR gamma. Journal of Cellular Biochemistry, 112, 2490–2501.

Conrad, D. J., Kuhn, H., Mulkins, M., Highland, E., & Sigal, E. (1992). Specific inflammatory cytokines regulate the expression of human monocyte 15-lipoxygenase. Proceedings of the National Academy of Sciences, 89(1), 217-221.

Cuzzocreaa, S., Pisanob, B., Dugoa, L., Ianarob, A., Maffiab, P., Patel, N.S.A., Di Paolaa, R., Ialentib, A., Genovesea, T., Chatterjeec, P.K., Di Rosab, M., Caputi, A.P., Thiemermann, C. (2004). Rosiglitazone, a ligand of the peroxisome proliferator-activated receptor-g, reduces acute inflammation. European Journal of Pharmacology, 483, 79-93.

Dix, T. A., & Aikens, J. (1993). Mechanisms and biological relevance of lipid peroxidation initiation. Chemical research in toxicology, 6(1), 2-18.

Dönmez, Y., Akhmetova, L., İşeri, Ö. D., Kars, M. D., & Gündüz, U. (2011). Effect of MDR modulators verapamil and promethazine on gene expression levels of MDR1 and MRP1 in doxorubicin-resistant MCF-7 cells. Cancer chemotherapy and pharmacology, 67(4), 823-828.

Donmez, Y., Gunduz, U. (2011). Reversal of multidrug resistance by small interfering RNA (siRNA) in doxorubicin-resistant MCF-7 breast cancer cells. Biomedicine and Pharmacotherapy, 65(2), 85-89.

Dos Santos, S.M., Weber, C., Franke, C., Muller, W.E., Eckert, G.P. (2007). Cholesterol: Coupling between membrane microenvironment and ABC transporter activity. Biochemical and Biophysical Research Communications, 354, 216–221.

Ejendal, K. F. K., Hrycyna, C. A. (2002). Multidrug resistance and cancer: the role of the human ABC transporter ABCG2. Current Protein & Peptide Science, 3(5), 503-511.

Erdem, M. (2014). Synthesis and characterization of polyethylene glycol coated magnetic nanoparticles and their use for anti-cancer drug delivery (Master's thesis, MIDDLE EAST TECHNICAL UNIVERSITY).

Funk, C. D., Chen, X. S., Johnson, E. N., & Zhao, L. (2002). Lipoxygenase genes and their targeted disruption. Prostaglandins & other lipid mediators, 68, 303-312.

Gao, J., Aksoy, B. A., Dogrusoz, U., Dresdner, G., Gross, B., Sumer, S. O., ... & Cerami, E. (2013). Integrative analysis of complex cancer genomics and clinical profiles using the cBioPortal. Sci. Signal., 6(269), pl1-pl1.

Gaschler, M.M., Stockwell B.R. (2017). Lipid peroxidation in cell death. Biochemical and Biophysical Research Communications, 482(3), 419-425.

Gillmor, S. A., Villaseñor, A., Fletterick, R., Sigal, E., & Browner, M. F. (1997). The structure of mammalian 15-lipoxygenase reveals similarity to the lipases and the determinants of substrate specificity. Nature structural biology, 4(12), 1003-1009.

Glück, S. (2005). Adjuvant chemotherapy for early breast cancer: optimal use of epirubicin, The Oncologist, 10, 780-791.

Gottesman, M. M., Fojo, T., Bates, Susan E. (2002). Multidrug resistance in cancer: role of ATP-dependent transporters. Nature Reviews Cancer, 2(1), 48-58.

Haeggström, J. Z., & Funk, C. D. (2011). Lipoxygenase and leukotriene pathways: biochemistry, biology, and roles in disease. Chemical reviews, 111(10), 5866-5898.

Hanahan, D., Weinberg, R. A., Francisco, S. (2000). The Hallmarks of Cancer Review. Cell, 100, 57-70.

Hanahan, D., & Weinberg, R. A. (2011). Hallmarks of cancer: the next generation. Cell, 144(5), 646-74.

Hendrich, A.B., Michalak, K. (2003). Lipids as a target for drugs modulating multidrug resistance of cancer cells. Current Drug Targets, 4, 23-30.

Holohan, C., Schaeybroeck, S.V., Longley, D.B., Johnston, P.G. (2013). Cancer drug resistance: an evolving paradigm. Nature Reviews Cancer, 13, 714-726.

Housman, G., Byler, S., Heerboth, S., Lapinska, K., Longacre, M., Snyder, N., Sarkar, S. (2014). Drug resistance in cancer: an overview. Cancers, 6, 1769-1792.

Iseri, O.D., Kars, M.D., Arpaci, F., Gunduz, U. (2010). Gene expression analysis of drug-resistant MCF-7 cells: implications for relation to extracellular matrix proteins. Cancer Chemotherapy and Pharmacology, 65(3), 447-455.

Ivanov I., Kuhn H., Heydeck D. (2015). Structural and functional biology of arachidonic acid 15-lipoxygenase-1 (ALOX15). Gene, 573, 1-32.

Jiang, W.G., Watkins, G., Douglas-Jones, A., Mansel, R.E. (2006). Reduction of isoforms of 15-lipoxygenase (15-LOX)-1 and 15-LOX-2 in human breast cancer. Prostaglandins, Leukotrienes & Essential Fatty Acids, 74(4), 235-45.

Jin, M. S., Oldham, M. L., Zhang, Q., & Chen, J. (2012). Crystal structure of the multidrug transporter P-glycoprotein from Caenorhabditis elegans. Nature, 490(7421), 566.

Jögi, A., Vaapil, M., Johansson, M., & Påhlman, S. (2012). Cancer cell differentiation heterogeneity and aggressive behavior in solid tumors. Upsala journal of medical sciences, 117(2), 217-224.

Kars, M.D., Iseri, O.D., Gunduz, U., Ural, A.U., Arpaci, F., Molnar, J. (2006). Development of rational in vitro models for drug resistance in breast cancer and modulation of MDR by selected compounds. Anticancer Research, 26, 4559-68.

Kars, M.D., Iseri, Ö.D., Ural, A.U., Gunduz, U. (2007). In vitro evaluation of zoledronic acid resistance developed in MCF-7 cells. Anticancer research, 27(6B), 4031-4037.

Kars, M.D., Iseri, O.D., Gunduz, U. (2011). A microarray based expression profiling of paclitaxel and vincristine resistant MCF-7 cells. European Journal of Pharmacology, 657(1-3), 4-9

Karukstis, K.K., Thompson, E.H.Z., Whiles, J.A., Rosenfeld, R.J. (1998). Deciphering the fluorescence signature of daunomycin and doxorubicin. Biophysical Chemistry, 73(3), 249-263.

Kazan, H. H., Urfali-Mamatoglu, C., Yalcin, G. D., Bulut, O., Sezer, A., Banerjee, S., & Gunduz, U. (2019). 15-LOX-1 has diverse roles in the resensitization of resistant cancer cell lines to doxorubicin. Journal of cellular physiology.

Keppler, D. (2011). Multidrug resistance proteins (MRPs, ABCCs): importance for pathophysiology and drug therapy. In Drug Transporters (pp. 299-323). Springer, Berlin, Heidelberg.

Kerjaschki, D., Bago-Horvath, Z., Rudas, M., et al. (2011). Lipoxygenase mediates invasion of intrametastatic lymphatic vessels and propagates lymph node metastasis of human mammary carcinoma xenografts in mouse. The Journal of Clinical Investigation, 121(5), 2000-12. doi: 10.1172/JCI44751.

Kuhn, H., Banthiya, S., & van Leyen, K. (2015). Mammalian lipoxygenases and their biological relevance. Biochimica et Biophysica Acta (BBA)-Molecular and Cell Biology of Lipids, 1851(4), 308-330.

Krishna, R., Mayer, L. D. (2000). Multidrug resistance (MDR) in cancer: mechanisms, reversal using modulators of MDR and the role of MDR modulators in influencing the pharmacokinetics of anti-cancer drugs. European Journal of Pharmaceutical Sciences, 11(4), 265-83.

Kudoh, K., Ramanna, M., Ravatn, R., Elkahloun, A.G., Bittner, M.L., Meltzer, P.S., Trent, J.M., Dalton, W.S., Chin, K. (2000). Monitoring the expression profiles of doxorubicin-induced and doxorubicin resistant cancer cells by cDNA microarray. Cancer Research, 60, 4161-66.

Lavie, Y., & Liscovitch, M. (2000). Changes in lipid and protein constituents of rafts and caveolae in multidrug resistant cancer cells and their functional consequences. Glycoconjugate journal, 17(3-4), 253-259.

Leibovici, J., Klein, O., Wollman, Y., Donin, N., Mahlin, T., & Shinitzky, M. (1996). Cell membrane fluidity and adriamycin retention in a tumor progression movel of AKR lymphoma. Biochimica et Biophysica Acta (BBA)-Biomembranes, 1281(2), 182-188.

Lima, R.T., Guimaraes, J.E., Vanconcelos, M.H. (2007). Overcoming K562Dox resistance to STI571 (Gleevec) by downregulation of P-gp expression using siRNAs. Cancer Therapy, 5, 67-76.

Livak, K.J., Schmittgen, T.D. (2001). Analysis of relative gene expression data using real-time quantitative PCR and the $2-\Delta\Delta CT$ method. Methods, 25, 402-408.

Longley, D. B., Johnston, P. G. (2005). Molecular mechanisms of drug resistance. The Journal of Pathology, 205(2), 275-292.

Mayer, L. D., Bally, M. B., & Cullis, P. R. (1986). Uptake of adriamycin into large unilamellar vesicles in response to a pH gradient. Biochimica Et Biophysica Acta (BBA)-Biomembranes, 857(1), 123-126.

Moussalli, M.J., Wu, Y., Zuo, X., Yang, X.L., Wistuba, I.I., Raso, M.G., Morris, J.S., Bowser, J.L., Minna, J.D., Lotan, R., Shureiqi, I. (2011). Mechanistic contribution of ubiquitous 15-lipoxygenase-1 expression loss in cancer cells

to terminal cell differentiation evasion. Cancer Prevention Research, 4(12), 1961-1972.

O'Prey, J., & Harrison, P. R. (1995). Tissue-specific regulation of the rabbit 15-lipoxygenase gene in erythroid cells by a transcriptional silencer. Nucleic acids research, 23(18), 3664-3672.

O'Shaughnessy, J. (2005). Extending survival with chemotherapy in metastatic breast cancer. The Oncologist, 10, 3(3), 20-9.

Ostareck, D.H., Ostareck-Lederer, A., Wilm, M., Hiele, B.J., Mann, M., et al. (1997). mRNA silencing in erythroid differentiation: hnRNP K and hnRNP E1 regulate 15-lipoxygenase translation from the 3' end. Cell, 89(4), 597-606.

Ostareck-Lederer, A., Ostareck, D.H., Standart, N., Hiele, B.J. (1994). Translation of 15- lipoxygenase mRNA is inhibited by a protein that binds to a repeated sequence in the 3' untranslated region. The EMBO Journal, 13,1476-1481.

Pallarés-Trujillo, J. A. V. I. E. R., López-Soriano, F. J., & Argilés, J. M. (2000). Lipids: a key role in multidrug resistance? International journal of oncology, 16(4), 783-881.

Palmer, T. D., Ashby, W. J., Lewis, J. D., & Zijlstra, A. (2011). Targeting tumor cell motility to prevent metastasis. Advanced drug delivery reviews, 63(8), 568-581.

Panda, M., & Biswal, B. K. (2019). Cell signalling and cancer: A mechanistic insight into drug resistance. Molecular biology reports, 1-15.

Peetla, C., Bhave, R., Vijayaraghavalu, S., Stine, A., Kooijman, E., & Labhasetwar, V. (2010). Drug resistance in breast cancer cells: biophysical characterization of and doxorubicin interactions with membrane lipids. Molecular pharmaceutics, 7(6), 2334-2348.

Peetla, C., Vijayaraghavalu, S., & Labhasetwar, V. (2013). Biophysics of cell membrane lipids in cancer drug resistance: Implications for drug transport and drug delivery with nanoparticles. Advanced drug delivery reviews, 65(13-14), 1686-1698.

Rieger, P. (2004). The biology of cancer genetics. Seminars in Oncology Nursing, 20(3), 145-154.

Rise, P., Eligini, S., Ghezzi, S., Colli, S., Galli, C. (2007). Fatty acid composition of plasma, blood cells and whole blood: relevance for the assessment of the fatty acid status in humans. Prostaglandins, Leukotrienes & Essential Fatty Acids, 76(6), 363-369.

Rodriguez, L.G., Wu, X., Guan, JL. (2005). Wound-Healing Assay. In: Guan JL. (eds) Cell Migration. Methods in Molecular Biology, 294. Humana Press.

Sade, A., Tuncay, S., Cimen, I., Severcan, F., Banerjee, S. (2012). Celecoxib reduces fluidity and decreases metastatic potential of colon cancer cell lines irrespective of COX-2 expression. Bioscience Reports, 32(1), 35-44. doi: 10.1042/BSR20100149.

Schneider, C.A., Rasband, W.S., Eliceiri, K.W. (2012). NIH Image to ImageJ: 25 years of image analysis. Nature Methods, 9, 671–675.

Sharom, F.J. (1997). The P-glycoprotein multidrug transporter: interactions with membrane lipids, and their modulation of activity. Biochemical Society Transactions, 25, 1088-96.

Sharom, F.J. (2014). Complex interplay between the P-glycoprotein multidrug efflux pump and the membrane: its role in modulating protein function. Frontiers in Oncology, 4, 1-19.

Shureiqi, I., Chen, D., Lee, J. J., Yang, P., Newman, R. A., Brenner, D. E., ... & Lippman, S. M. (2000). 15-LOX-1: a novel molecular target of nonsteroidal anti-inflammatory drug-induced apoptosis in colorectal cancer cells. Journal of the National Cancer Institute, 92(14), 1136-1142.

Shureiqi, I., Lippman, S.M. (2001). Lipoxygenase modulation to reverse carcinogenesis. Cancer Research, 61(17), 6307-12.

Shureiqi, I., Zuo, X., Broaddus, R., Wu, Y., Guan, B., Morris, J. S., & Lippman, S. M. (2007). The transcription factor GATA-6 is overexpressed in vivo and contributes to silencing 15-LOX-1 in vitro in human colon cancer. The FASEB Journal, 21(3), 743-753.

Simon, S. M., Schindler, M. (1994). Cell biological mechanisms of multidrug resistance in tumours, Proc Natl Acad Sci USA, 91(9), 3497-3504.

Sinicrope, F.A., Dudeja, P.K., Bissonnette, B.M., Safa, A.R., Brasitus, T.A. (1992). Modulation of P-glycoprotein-mediated drug transport by alterations in lipid fluidity of rat liver canalicular membrane vesicles. Journal of Biological Chemistry, 267(35), 24995-5002.

Smith, G., Glaser, M., Perumal, M., Nguyen, Q., Shan, B., Arstad, E., Aboagye, E.O. (2008). Design, synthesis, and biological characterization of a Caspase 3/7 selective isatin labeled with 2-[18F]fluoroethylazide. Journal of Medicinal Chemistry, 51, 8057–67.

Sturlan, S., Baumgartner, M., Roth, E., & Bachleitner-Hofmann, T. (2003). Docosahexaenoic acid enhances arsenic trioxide–mediated apoptosis in arsenic trioxide–resistant HL-60 cells. Blood, 101(12), 4990-4997.

Taraboletti, G., Perin, L., Bottazzi, B., Mantovani, A., Giavazzi, R., Salmona, M. (1989). Membrane fluidity affects tumor-cell motility, invasion and lung-colonizing potential. International Journal of Cancer, 44(4), 707-713.

Tavakoli-Yaraki, M., Karami-Tehrani, F. (2013). Apoptosis Induced by 13-S-hydroxyoctadecadienoic acid in the Breast Cancer Cell Lines, MCF-7 and MDA-MB-231. Iranian Journal of Basic Medical Sciences, 16(4), 653-659.

Thiele, B. J., Berger, M., Huth, A., Reimann, I., Schwarz, K., & Thiele, H. (1999). Tissue-specific translational regulation of alternative rabbit 15-lipoxygenase

mRNAs differing in their 3′-untranslated regions. Nucleic acids research, 27(8), 1828-1836.

Tian, R., Zuo, X., Jaoude, J., Mao, F., Colby, J., Shureiqi, I. (2017). ALOX15 as a suppressor of inflammation and cancer: Lost in the link. Prostaglandins & Other Lipid Mediators, 132, 77–83.

Tsuruo, T., Naito, M., Tomida, A., Fujita, N., Mashima, T., Sakamoto, H., Haga, N. (2003). Molecular targeting therapy of cancer: drug resistance, apoptosis and survival signal. Cancer Science, 94(1), 15-21.

Tuncer, S., Keskus, A.G., Colakoglu, M., Cimen, I., Yener, C., Konu, O., Banerjee, S. (2017). 15-Lipoxygenase-1 re-expression in colorectal cancer alters endothelial cell features through enhanced expression of TSP-1 and ICAM-1. Cellular Signaling, 39, 44-54.

Urfali-Mamatoglu, C., Kazan, H.H., Gunduz, U. (2018). Dual function of programmed cell death 10 (PDCD10) in drug resistance. Biomedicine and Pharmacotherapy, 101, 129-136.

Walther, M., Anton, M., Wiedmann, M., Fletterick, R., Kuhn, H. (2002). The N-terminal domain of the reticulocyte-type 15-lipoxygenase is not essential for enzymatic activity but contains determinants for membrane binding. Journal of Biological Chemistry, 277(30), 27360-66.

Wan Seok Yang, W.S., Kim, K.J., Gaschler, M.M., Patel, M., Shchepinov, M.S., Stockwell, B.R. (2016). Peroxidation of polyunsaturated fatty acids by lipoxygenases drives ferroptosis. Proceedings of the National Academy of Sciences of the USA, 113(34), E4966-75.

Yamamoto, Y., Yoshioka, Y., Minoura, K. et al. (2011) An integrative genomic analysis revealed the relevance of microRNA and gene expression for drug-resistance in human breast cancer cells. Molecular Cancer, 10, 1-16.

Young, L., Sung, J. Stacey, G., Masters, J.R. (2010). Detection of Mycoplasma in cell cultures. Nature Protocols, 5(5), 929-34.

APPENDICES

A. Ingredients of Solutions

A.1. Phosphate Buffered Saline (pH 7.2)

1 PBS tablet (Sigma, Germany) was dissolved in 100ml distilled water and autoclaved at 121°C for 20 minutes.

A.2. 4X Separating Buffer

91 g Tris base (Bioshop)

2 g SDS (Applichem)

Volume is completed to 500 ml with distilled water, after adjusting pH to 8.8.

A.3. 4X Stacking Buffer

30.35g Tris base (Bioshop)

2 g SDS (Applichem)

After pH was adjusted to 6.8, volume is completed to 500 ml with distilled water.

A.4. Running Buffer

100ml Tris-Glycine buffer (10X)

890ml distilled water

10 Ml of 10% SDS solution

A.6.   4X Sample Loading Buffer

2.0 ml 1M Tris-HCl (pH 6.8)

0.8 g SDS

4.0 ml of 100% glycerol

1.0 ml of 0.5 M EDTA

8.0 mg bromophenol blue

2.6 ml distilled H_2O

The buffer is aliquoted in 96 µl and stored at -20°C at dark. Before experimentation, 4 µl of 17.4 M beta-merchaptoethanol (Amresco) is added to each aliquot and mixed well.

A.7.   5X Bradford Reagent

100 mg Coomassie G-250 (Serva)

47 ml methanol

100 ml of 85% phosphoric acid (Riedel-de Haen)

Volume is completed to 200 mL with distilled water and stored at 4°C at dark.

A.8.   10X TBS Buffer

24.23 g Tris.HCl

80.06 g NaCl

After pH was adjusted to 7.6, volume was completed to 1000 ml with distilled water. TBS is autoclaved at 121°C for 20 minutes

A.9.   TBST (0.1% Tween 20)

100 ml of 10X TBS

900ml distilled water

1 ml of Tween 20 (Amresco)

A.10. Blocking Buffer

0.5 g skimmed milk (Amresco) or BSA was dissolved in 10 ml of 0.1% TBST.

A.11. 10X Tris-Glycine Buffer

30.3 g Tris base

144.1 g Glycine (Bioshop)

After pH was adjusted to 8.3, volume was completed to 1000 ml with distilled water.

A.12. Transfer buffer

100 ml of 10X Tris-Glycine buffer

5 ml of 10% SDS solution

800 ml Methanol (Sigma)

Volume was completed to 1000 ml with distilled water.

A.13. Stripping buffer

0.76 g Tris base

2 g SDS

700 µl of beta-merchaptoethanol

After pH was adjusted to 6.8, volume was completed to 1000 ml with distilled water.

B. The Preliminary Data for Possible Novel Trasncript Variant of *ALOX15*

The first studies on qRT-PCR primer pair to see the expression level of *ALOX15* in cell lines has been designed to amplify an amplicon in the exon-exon junction (Exon 10 and 11 according to transcript variant ENST00000293761.7; Figure B1). This primer pair was obtained form Dr. Banerjee's Lab. Under optimized conditions where there is not any genomic DNA contamination, these primers are expected to amplify a region including just exons (a 100 bp amplicon from exon 10 and 11 according to ENST00000293761.7).

Figure B.0-1 The sequence showing primer pair in the first qRT-PCR studies. Red sequence: Forward primer; green sequence: Reverse primer. Sequence obtained from Ensembl.org (ENST00000293761.7).

In qRT-PCR studies, it has been realized that these primers amplified more than one amplicon. Conventional PCR studies also confirmed this observation. According to PCR results where a genomic DNA was used as control, one of the unintended PCR bands overlapped with that of genomic DNA control, pointing that the intronic region (intron 10 according to ENST00000293761.7; Figure B1) was not excluded from the mRNA. This result would be a result of genomic DNA contamination to cDNAs used in the PCR experiments. To test the possible genomic DNA contamination, DNase-treated RNA samples by which cDNAs have been synthesized were used in PCR by *ACTB* primers. According to results (Figure B2), there were not any bands for DNase-treated RNA samples, figuring that there was

not DNA contamination in DNase-treated RNA samples. Still, firstly used ALOX15 primers amplified an amplicon possibly including intronic region (Figure B2). These results have been deciphered as a novel transcript variant of *ALOX15* and further studies were designed in this perspective. There are seven reported transcript variant of *ALOX15*, five of which encodes a protein (ensemble.org). Moreover, the expression of those putative variant was shown to be different according to convenient PCR results, where the band pointing possible intronic region-containing amplicon was thicker in MCF7 DOX cells compared to sensitive counterpart (Figure B2).
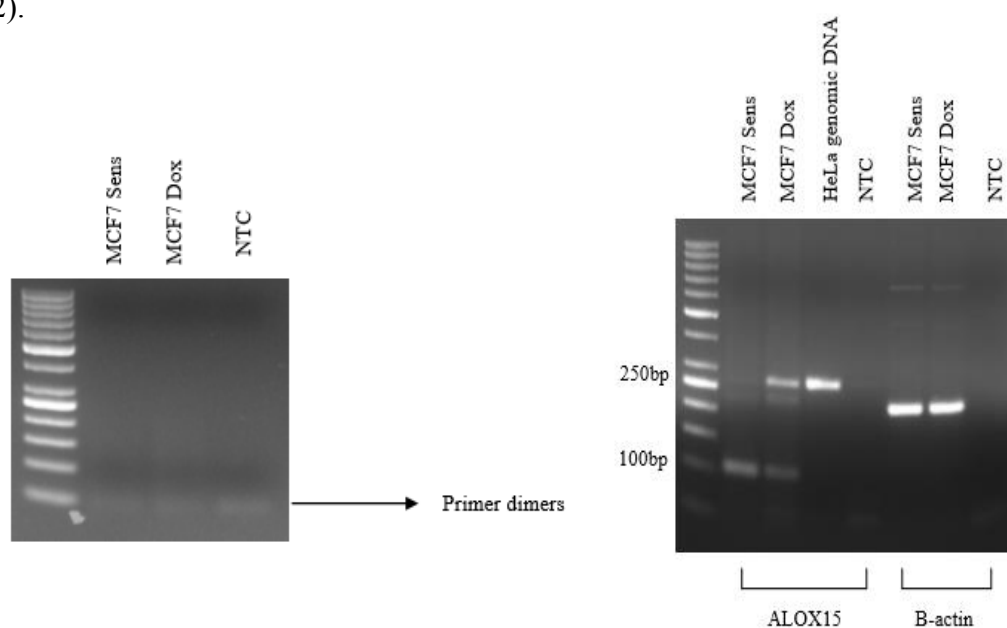

Figure B.0-2 Conventional PCR studies for assessing possible genomic DNA contamination in DNase-treated RNA samples (left) and for showing that firstly used ALOX15 primers amplified more than one PCR bands, one of which overlaps with that of intronic-region containing genomic DNA control (rigth).

According to results given above (Figure B2), a new statement would be proposed as *ALOX15* would have a novel transcript variant whose differential expression would be related to resistance to anticancer drugs.

To be able to further analyse the possible transcript variant of ALOX15, two new set of primers were designed just inside the intronic region (Figure B3) to eliminate the possible primer-specific problems and show that the intronic region is really inside the mRNA. These primers (iFP and iRP) was used with the combination of firstly designed primers (oFP and oRP) to be able to obtain amplicons with optimal length (~200 bp) and annealing temperature ($59^{o}C$) which is the working temperature for firstly used primer pair.
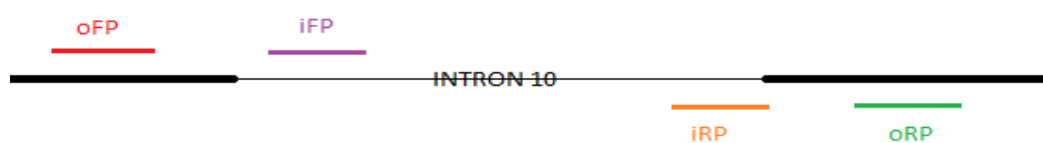
Figure B.0-3 Illustration for primer binding sites on ALOX15. oFP: exonic forward primer; oRP exonic reverse primer; iFP: intronic forward primer; iRP: intronic reverse primer.

In addition to firstly designed primers (oFP+oRP), newly designed primers were combined with those primers (iFP+oRP and oFP+iRP) and cDNAs were proved to be synthesized from RNA samples without genomic DNA contamination. According to conventional PCR results, intronic region was definitely inside the cDNAs obtained HeLa sensitive, MCF7 sensitive and MCF7 DOX cells (Figure B4). Surprisingly, bands for intronic region-containing amplicon were thicker in MCF7 sensitive cells compared to MCF7 DOX cells, which was the reverse with the firstly used primers (oFP+oRP).
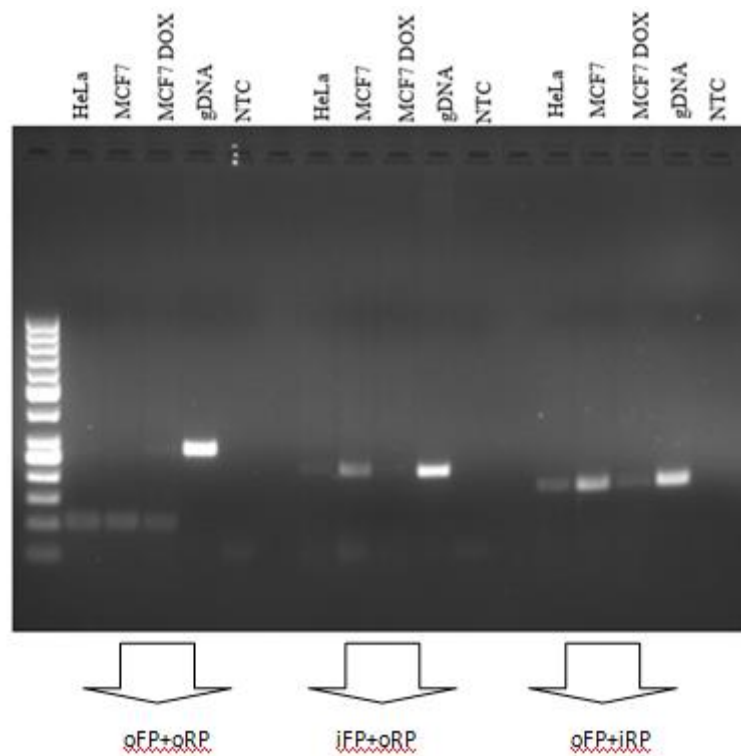
Figure B.0-4 Conventional PCR results with firstly used and newly designed intronic regions for cDNAs obtained from HeLa, MCF7 and MCF7 DOX cells in the presence of genomic DNA control (gDNA).

To further prove that the intronic region was obtained from mRNAs, RNA samples were treated with RNase A. After RNase A and DNase treatments, the expectation was to obtain no bands from the so called "cDNAs". Figure B5 proves that RNase A was able to digest all of the RNAs obtained from HeLa, MCF7 and MCF7 DOX.

99
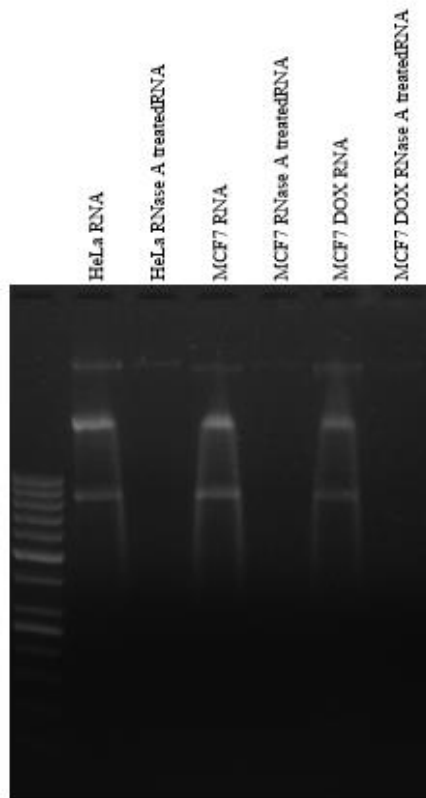
Figure B.0-5 Effect of RNase A treatment on RNA samples.

Next, both RNase A-treated and non-treated RNA samples were treated with DNase and those samples were used for cDNA synthesis. Then, a conventional PCR where *ACTB* primers were used was set by these cDNAs. According to results (Figure B6), there were no bands for RNase- and DNase-treated "cDNAs", pointing that all the bands were obtained from mRNA-converted cDNAs.
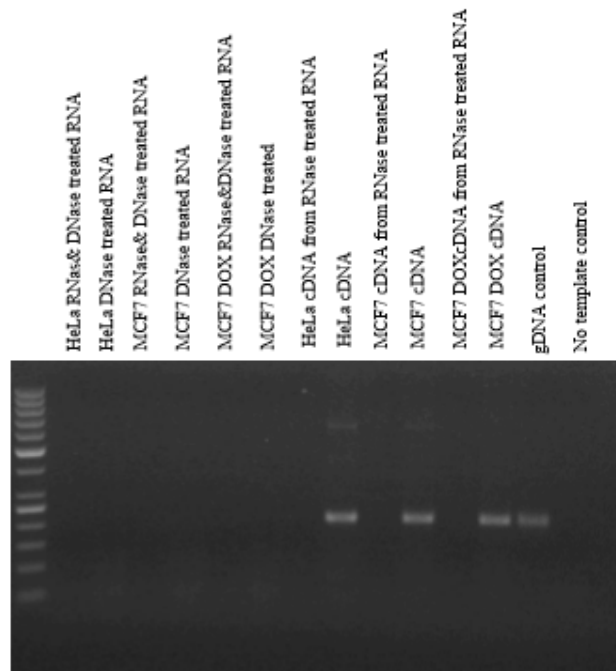
Figure B.0-6 Conventional PCR result after RNase and DNase treatments.

As a next step, related intronic sequence was scanned in public RNA-seq data for MCF7 cell line via Sequence Read Archive (SRA) database of NCBI (ncbi.nlm.nih.gov/sra). SRA is a database which allows users to blast a query in RNA-seq data. In an experiment where four different runs (two estradiol-treated and two non-treated) were conducted for RNA-seq for MCF7 cell line, related intronic sequence was blasted. According to result, the query was part-by-part but totally aligned in the reads of RNA-seq for MCF7 cells (Figure B7). Next generation sequencing strategies are based on sequencing DNA or RNA with short lengths. Thus, it was not surprising that all intronic sequence was not aligned in just one read. After alignment, moreover, SRA database allow users to see the aligned reads in the nucleotide level. Figure B8 shows the reads where query was aligned with high score. According to these data mining results, it can be strongly proposed that the intronic sequence would be located in mRNA, pointing a possible transcript variant of *ALOX15* as a result of putative alternative splicing mechanism where the related intron was used as an exon.
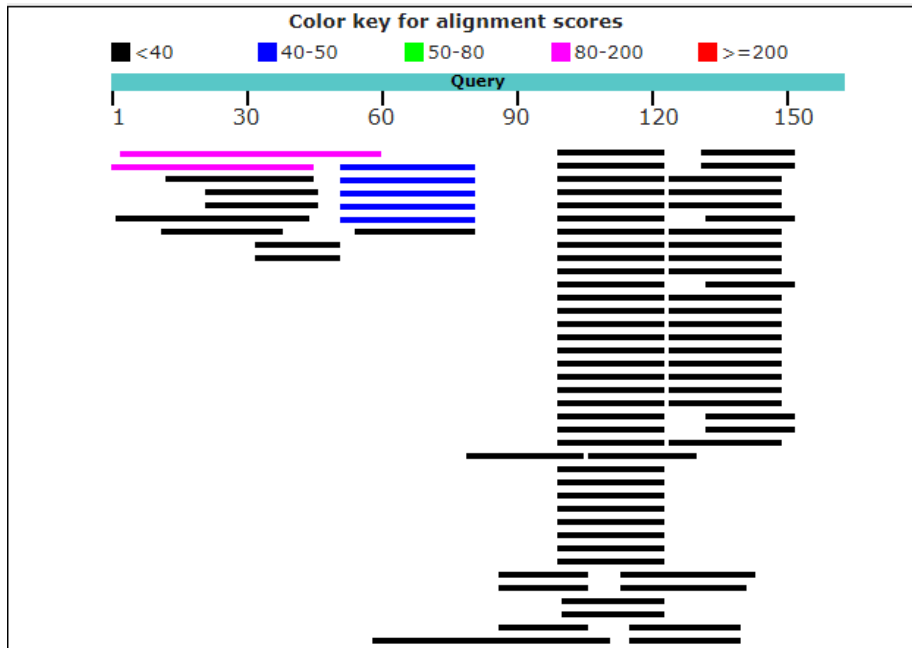
Figure B.0-7 Alignment result of the blasting of the related intronic sequence in RNA-seq for MCF7 cells.

Figure B.0-8 Reads that aligned to the intronic sequence with high score.

CURRICULUM VITAE

Personal Details

Name : Hasan Hüseyin

Surname : Kazan

Nationality : Turkish

DOB : 13 Dec. 1989

Address : İşçi Blokları Mah. 425. Sok. 122/1 06520 Çankaya, Ankara, TURKEY

Mobile : +90 554 207 85 38

E-mail : hasanhuseyinkazan@gmail.com

Languages

Turkish (Native)

English (Advance)

Spanish (Beginner)

Computer Skills

Microsoft Office, MatLab, Web-based bioinformatic tools, SerialCloner, ChemBio, UCSF Chimera, Jmol, GraphPad Prism, IVA Ingenuity, SPSS, SeqA6, GeneMapper.

Education

2003-2007 Darıca Neşet Yalçın High School (in English)

2007-2012 Undergraduate Program in Department of Molecular Biology and Genetics, Istanbul Technical University (ITU), Istanbul, Turkey

2012-2015 Master of Science Program in Department of Biotechnology, Middle East Technical University (METU), Ankara, Turkey

2015- PhD Program in Biology Department, Middle East Technical University (METU), Ankara, Turkey

Business Experience

Research assistant at Middle East Technical University Central Laboratory

Molecular Biology and Biotechnology R& D Unit, 2013-2015.

Kit developer and producer at Matrix Biotek, Inc. Gazi University Technocity, Ankara, Turkey, 2016.

Laboratory worker at the Department of Medical Genetics, Faculty of Medicine, Gazi University, Ankara, Turkey, 2017-.

Laboratory Techniques

Molecular cloning, PCR, cell culture, recombinant protein production, qPCR, Western Blotting, immunocytochemistry, fluorescence assays, fluorescence microscopy, transient-stable transfection, Sanger Sequencing, Next Generation Sequencing (Ion PGM, Ion S5), human tissue processing (DNA isolation and culturing), MLPA, STR and Fragile X analyses.

Scholarships/Awards

2211-C Program, The Scientific and Technological Research Council of Turkey, 2017-.

Winner of Young Entrepreneur Competition, Gebze Technical University, 2017.

Research Interests

Molecular medicine, molecular mechanisms of cancer and drug resistance, lipid metabolism